AFGL-TR-89-0016

Determination of Local Empirical Covariance Functions From Residual Terrain Reduced Altimeter Data

Per Knudsen

Ohio State University
Department of Geodetic Science
and Surveying
Columbus, OH 43210

November 1988

Scientific Report No. 5

APPROVED FOR PUBLIC RELEASE; DISTRIBUTION UNLIMITED

AIR FORCE GEOPHYSICS LABORATORY
AIR FORCE SYSTEMS COMMAND
UNITED STATES AIR FORCE
HANSCOM AIR FORCE BASE, MASSACHUSETTS 01731-5000

This technical report has been reviewed and is approved for publication.

CHRISTOPHER JEKELI
Contract Manager

THOMAS P. ROONEY, Chief
Geodesy & Gravity Branch

FOR THE COMMANDER

DONALD H. ECKHARDT, Director
Earth Sciences Division

Qualified requestors may obtain additional copies from the Defense Technical Information Center.

If your address has changed, or if you wish to be removed from the mailing list, or if the addressee is no longer employed by your organization, please notify AFGL/DAA, Hanscom AFB, MA 01731-5000. This will assist us in maintaining a current mailing list.

Do not return copies of this report unless contractual obligations or notices on a specific document requires that it be returned.

Unclassified
SECURITY CLASSIFICATION OF THIS PAGE

REPORT DOCUMENTATION PAGE

Form Approved OMB No. 0704-0188

1a. REPORT SECURITY CLASSIFICATION: Unclassified	1b. RESTRICTIVE MARKINGS
2a. SECURITY CLASSIFICATION AUTHORITY	3. DISTRIBUTION/AVAILABILITY OF REPORT: Approved for public release; distribution Unlimited
2b. DECLASSIFICATION/DOWNGRADING SCHEDULE	
4. PERFORMING ORGANIZATION REPORT NUMBER(S): OSU/DGSS Report No. 395	5. MONITORING ORGANIZATION REPORT NUMBER(S): AFGL-TR-89-0016
6a. NAME OF PERFORMING ORGANIZATION: Department of Geodetic Science and Surveying; 6b. OFFICE SYMBOL (If applicable)	7a. NAME OF MONITORING ORGANIZATION: Air Force Geophysics Laboratory
6c. ADDRESS (City, State, and ZIP Code): The Ohio State University, Columbus, Ohio 43210	7b. ADDRESS (City, State, and ZIP Code): Hanscom AFB, Massachusetts 01731-5000
8a. NAME OF FUNDING/SPONSORING ORGANIZATION; 8b. OFFICE SYMBOL (If applicable)	9. PROCUREMENT INSTRUMENT IDENTIFICATION NUMBER: F 19628-86-K-0016
8c. ADDRESS (City, State, and ZIP Code)	10. SOURCE OF FUNDING NUMBERS

PROGRAM ELEMENT NO.	PROJECT NO.	TASK NO.	WORK UNIT ACCESSION NO.
62101F	7600	03	AQ

11. TITLE (Include Security Classification): Determination of Local Empirical Covariance Functions From Residual Terrain Reduced Altimeter Data

12. PERSONAL AUTHOR(S): Per Knudsen

13a. TYPE OF REPORT	13b. TIME COVERED	14. DATE OF REPORT (Year, Month, Day)	15. PAGE COUNT
Scientific No. 5	FROM _____ TO _____	1988 November	66

16. SUPPLEMENTARY NOTATION

17 COSATI CODES			18. SUBJECT TERMS (Continue on reverse if necessary and identify by block number)
FIELD	GROUP	SUB-GROUP	geodesy; gravity; least-squares collocation

19. ABSTRACT (Continue on reverse if necessary and identify by block number)

Local empirical covariance functions have been estimated from cross-over adjusted high-pass filtered SEASAT/GEOS-3 altimeter data in three local 2° x 2° areas in the North Atlantic ocean. The high-pass filtering was needed in order to remove remaining long wavelength parts of the gravity field due to errors in the spherical harmonic expansion that was used, and effects from sea surface topography and correlated parts of radial orbit errors. After a subtraction of noise variances geoid height variances associated with harmonic degrees above 180 of 0.213 m^2, 0.112 m^2, and 1.217 m^2 were obtained in the three local areas respectively.

Then residual terrain effects were computed from Airy-Heiskanen isostatic earth models using Fourier techniques and "SYNBAPS" bathymetry. The depths of compensation were increased in order to simulate regional Vening Meinesz models. Comparisons of altimetric and bathymetric geoid heights showed that the magnitudes of the unmodelled parts of the gravity fields practically were unaffected by changes in the depths of

20. DISTRIBUTION/AVAILABILITY OF ABSTRACT	21. ABSTRACT SECURITY CLASSIFICATION
☒ UNCLASSIFIED/UNLIMITED ☐ SAME AS RPT ☐ DTIC USERS	Unclassified

22a. NAME OF RESPONSIBLE INDIVIDUAL	22b. TELEPHONE (Include Area Code)	22c. OFFICE SYMBOL
Christopher Jekeli		AFGL/LWG

DD Form 1473, JUN 86 — Previous editions are obsolete. — SECURITY CLASSIFICATION OF THIS PAGE

compensation from 50 km to 70 km. Estimations of local empirical covariance functions from the terrain reduced altimetry showed that the geoid height variances were reduced by about 3 dB, 0 dB, and 9 dB to values of 0.096 m^2, 0.108 m^2, and 0.147 m^2 respectively. The variances have hereby decreased to about the same level.

Finally Tscherning/Rapp covariance function models were adjusted to fit the empirical covariance values. The results show that a determination of a covariance function model needs more information about the gravity field than provided by the altimetry, or strong generalizations about the gravity field. When terrain reduced quantities are considered, the major differences between the gravity fields are removed, which should make a determination of a covariance function model easier and decrease the effects of using a wrong covariance function. Assuming that the decay of the potential degree variances associated with the terrain reduced gravity field is -3.6, a covariance function model with $(R-R_B)$ = 3.0 km, $A = 711 \cdot 10^3$ $(m^2/s^2)^2$ having a gravity anomaly variance of $(15\ mgal)^2$ is suggested.

FOREWORD

This report was prepared by Per Knudsen, Research Associate, Dept. of Geodetic Science and Surveying, The Ohio State University, and Geodetic Institute, Denmark, under Air Force Geophysics Laboratory Contract No. F19628-86-K-0016, The Ohio State University Research Foundation Project 718188. This contract is administrated by Air Force Geophysics Laboratory, Hanscom Air Force Base, Massachusetts, with Dr. C. Jekeli, Scientific Program Officer.

Certain computer funds in the study were supplied by the Instruction and Research Computer Center through the Department of Geodetic Science and Surveying.

This report is a contribution to a gravity field modelling project supported in parts by the Danish Space Board and Norsk Hydro. The research was carried out while the author was on leave from the Geodetic Institute, Denmark. Travel support was provided by the Danish Research Academy, NATO Science Fellowship Program, and the Danish Space Board.

The author wishes to thank Professor R.H. Rapp and the rest of the department for hosting me at OSU and helping me and my family to get settled in Columbus. An additional thanks to Lisa Schneck for her typing of this report.

Table of Contents

List of Tables

List of Figures

Figure

Area 3 from 10′x10′ mean values of high-pass filtered altimeter data (0), residual terrain reduced altimeter data (x), and bathymetric geoid (+). The bathymetric geoid was calculated using a compensation depth of 70 km.

1. Introduction

In studies of the earth's anomalous gravity field, empirical covariance functions are of great interest. The behavior of the gravity field is reflected in these functions. The magnitude of the variations and the roughness of the field is described. This kind of information is important and has to be taken into account when gravity field related quantities are estimated from a set of observations. The method of least squares collocation (Moritz, 1980), is widely used for this purpose. The method needs a covariance function to express the relations between the observations and between the estimated quantities and the observations. The best least squares agreements with the true potential is obtained when the empirical covariance function is used.

Global empirical covariance values were estimated from gravity observations by Tscherning and Rapp (1974). They derived some covariance function models, and an expression for the global empirical covariance function was found.

When studies of the gravity field takes place in local areas, the use of high degree spherical harmonic approximations is very important. Estimations of gravity field related quantities are carried out relative to the spherical harmonic approximations using the residual observations and the local empirical covariance function. This procedure corresponds to the stepwise collocation (Moritz, 1980), where the solution of the first step is known.

The determination of a local empirical covariance function was discussed by Goad et al. (1984). They arrived at the following definition of a local covariance function: "A local covariance function is a special case of a global covariance function where the information content of wavelengths longer than the extent of the local area has been removed, and the information outside, but nearby, the area is assumed to vary in a manner similar to the

information within the area". They suggest that the Tscherning/Rapp models are used in order to adjust an expression to empirical values in a similar way as in the global case. This was done by Knudsen (1987) using an iterative least square inversion procedure. The empirical covariance values were determined from altimeter and gravity data relative to a spherical harmonic approximation of degree and order 180.

A different approach is to use the known part of the anomalous density distribution in the earth. The effect from the topography is a considerable part of the gravity field and, as far as the topography is known, this effect can be used when the gravity field is modelled. Results obtained by Forsberg (1984) show that the topographic effect is a large part of the short wavelength part of the gravity field. Furthermore, the results show that the gravity field becomes much more homogeneous when terrain reduced quantities from different local areas are evalueated. In these studies, a density contrast of 2670 kg/m^3 was assumed, but actual density contrasts could also be taken into account. This was done by Sünkel et al. (1987) when they computed terrain effects using both a digital terrain model and a digital density model.

Covariance functions are needed in estimation methods like least square collocation and they have to be consistent with the observations that are used. Unfortunately, the estimations of such functions is hampered by the lack of data in the areas where the gravity field modelling is to take place. Consequently, a covariance function model has to be chosen. It is, therefore, important to understand the variability of the local empirical covariance functions. The results mentioned above indicate that this variability decreases remarkably when the terrain effect is taken into acount. The residual gravity field becomes more homogeneous and the choice of a covariance function model becomes easier.

In this report, techniques for the estimation of empirical covariance functions are described. In order to show the importance of terrain reductions, previous results are summarized. Problems with centering observations are treated and a method for the determination of a covariance function model is described. New studies of the variability of the local empirical covariance functions are carried out in ocean areas using altimeter data along with bathymetry data. Terrain effects are calculated from the bathymetry and the role of an isostatic compensation of the ocean bottom topography is evaluated.

2. The Local Empirical Covariance Function

In this chapter the estimation and modelling of a local empirical covariance function are evaluated. The importance of a complete removal of wavelengths longer than the extent of the local area is pointed out, and a method for doing this consistently using different kinds of observations is given. Problems in using space domain or frequency domain methods for the estimation of a covariance function are treated, and the effect of noise associated with the observations is evaluated. Finally, an iterative least square inversion procedure for adjusting a covariance function model to fit empirical covariance values is described.

2.1 The local covariance function

In the following ΔT is the anomalous potential T where the information content of wavelengths longer than the extent of a local area $(\phi_1,\phi_2,\lambda_1,\lambda_2)$, T_{ref}, is subtracted. L and L´ are two linear functional associated with the observations $y=L(\Delta T)$ and $y'=L'(\Delta T)$ located at (ϕ,λ) and (ϕ',λ'). If the averages of y and y´ over the area are zero, then the local autocovariance of

y (if $L = L'$) or the local crosscovariance between y and y' is given by

$$C(\psi) = \frac{1}{A} \int_{\phi_1}^{\phi_2} \int_{\lambda_1}^{\lambda_2} \frac{1}{2\pi} \int_{0}^{2\pi} yy' d\alpha \cos(\phi)\, d\phi d\lambda \qquad (2.1)$$

where

$$\cos\psi = \sin\phi \sin\phi' + \cos\phi \cos\phi' \cos(\lambda-\lambda') \qquad (2.2)$$

A is the size of the area on a unit sphere,
α is the aximuth.

This rotational invariant representation of the covariance function is calculated as an average of the products yy' over the area (the two outer integrations) and an average over the azimuth (the inner integration). (Corresponding to homogeneity and isotropy respectively in a plane.) The integration over the local area is restricted to the observations y. When ψ goes from zero to π the observations of y' are used located over the whole sphere. (See also Tscherning, 1985, and Sanso, 1986).

In practice the observations are given in discrete points in the area and the calculation of the covariance function is then done by numerical integration (Tscherning and Rapp, 1974). If each observation y_i represents a small area A_i and y'_j represents an area A_j then

$$C_k = \frac{\sum A_i A_j y_i y'_j}{\sum A_i A_j} \qquad (2.3)$$

with

$$\psi_{k-1} < \psi_{ij} \leq \psi_k \qquad (2.4)$$

If the area is subdivided into small cells holding one observation each and A_i and A_j are assumed to be equal then equation (2.3) reduces to

$$C_k = \frac{\sum y_i y'_j}{N_k} \qquad (2.5)$$

where N_k is the number of products, $y_i y'_j$, in the k'th interval.

Suppose T is expanded into spherical harmonics, and a global gravity potential approximation up to degree and order N, T_N, is subtracted in order

to obtain ΔT. Then the covariance function, $K(\psi)$, associated with $(T-T_N)$ is expressed by a sum of a series of Legendre polynomials of order i, P_i, (Tscherning and Rapp, 1974, and Tscherning, 1986)

$$K(\psi) = \sum_{i=0}^{N} \varepsilon_i(T,T)\left(\frac{R^2}{rr'}\right)^{i+1} P_i(\cos\psi) + \sum_{i=N+1}^{\infty} \sigma_i(T,T)\left(\frac{R_B^2}{rr'}\right)^{i+1} P_i(\cos\psi) \tag{2.6}$$

where

$\varepsilon_i(T,T)$	are the potential error degree-variances,
$\sigma_i(T,T)$	are the potential degree-variances,
r,r'	are the radial distances of y and y',
R	is the mean earth radius, and
R_B	is the radius of a Bjerhammar sphere ($R_B^2 < rr'$).

The integer N, relative to the size of the local area, is supposed to fulfill the condition that $2\pi/N$ is smaller than the extention of the area where the local covariance function is determined. $(T-T_N)$ is equal to ΔT if an exact agreement between T_{ref} and T_N exists. Consequently, the error degree-variances are zero. The degree-variances are positive numbers and are related to the spherical power spectrum of the earth gravity field. It is well known that the degree-variances tend to zero somewhat faster than i^{-3} and that the Tscherning/Rapp (1974) model 4 is a reasonable choice for a degree-variance model,

$$\sigma_i(T,T) = A/((i-1)(i-2)(i+24)) \tag{2.7}$$

where A is a constant in units of $(m/s)^4$. For geoid heights, ζ, and gravity anomalies, Δg, we then have the degree variances associated with the respective auto- and cross-covariance functions (γ is the normal gravity)

$$\sigma_i(\zeta,\zeta) = 1/(\gamma\gamma')\sigma_i(T,T) \tag{2.8}$$
$$\sigma_i(\Delta g,\Delta g) = (i-1)^2/(rr')\sigma_i(T,T) \tag{2.9}$$
$$\sigma_i(\zeta,\Delta g) = (i-1)/(\gamma r')\sigma_i(T,T) \tag{2.10}$$

See Tscherning (1976) for degree-variances associated with other gravity field related quantities.

In a flat earth approximation the sphere is replaced by a plane and (ϕ,λ,ψ) is replaced by (x,y,s) where $s^2=x^2+y^2$. The power spectral density, or, more loosely, the power spectrum of ΔT, $\phi(u,v)$, is then evaluated using a 2-dimensional Fourier transform. Let $\tilde{y}$ (and $\tilde{y}'$) be the Fourier transform of y (and y'), then

$$\tilde{y}(u,v) = \int_{-\infty}^{\infty}\int_{-\infty}^{\infty} y(x,y)e^{-i(ux+vy)}dxdy \qquad (2.11)$$

and $\phi_{LL'}(u,v)$ the power spectrum associated with y and y'

$$\phi_{LL'}(u,v) = \tilde{y}(u,v)\ \tilde{y}'(u,v)* \qquad (2.12)$$

where $\tilde{y}'(u,v)*$ is the complex conjugate of $\tilde{y}(u,v)$.

The power spectrum of ΔT is then obtained from $\phi_{LL'}(u,v)$ in a similar way, as in the spherical case, by applying the inverse linear functionals related to y and y' on the spectrum. Then the 2-dimensional covariance function, K(x,y), is obtained using the inverse Fourier transform.

$$K(x,y) = \frac{1}{4\pi^2}\int_{-\infty}^{\infty}\int_{-\infty}^{\infty} \phi(u,v)e^{i(ux+vy)}dudv \qquad (2.13)$$

and the isotropic covariance function, K(s), by averaging over the azimuth

$$K(s) = \frac{1}{2\pi}\int_{0}^{2\pi} K(x,y)d\alpha \qquad (2.14)$$

Using this procedure the integrations in eq. (2.1) are calculated as a convolution first and then an average over the azimuth.

If the power spectrum, $\phi(u,v)$, is isotropic (or had become isotropic by averaging over the azimuth in the frequency domain) the isotropic covariance function K(s), is obtained from eq. (2.13) where the Fourier transform is reduced to an inverse Hankel transform. Consequently the isotropic power spectrum is obtained from the isotropic covariance function using a Hankel

transform (and not a 1-dimensional Fourier transform). That is

$$\Phi(\omega) = \int_0^\infty K(s) J_0(s\omega) s \, ds \qquad (2.15)$$

and

$$K(s) = \int_0^\infty \Phi(\omega) J_0(\omega s) \omega \, d\omega \qquad (2.16)$$

where $\omega^2 = u^2+v^2$ and J_0 is the Bessel function of order zero.

For details cf. Nash and Jordan (1978), Forsberg (1984a) and Schwarz (1985).

These formulas (2.11-2.16) are given in an infinite plane and the spectrum, given in eq. (2.12), is continuous, but it becomes discrete in the local case if periodicity is assumed. Then the integration in eq. (2.11) becomes finite and the integration in eq. (2.13) and (2.16) reduces to a summation. The discrete values of the spectrum appear for wavelengths $(x_2-x_1)/j$ and $(y_2-y_1)/k$ in each direction, when j and k are positive integers. On a sphere this corresponds to harmonic degree $2\pi*j/(x_2-x_1)$ and $2\pi*k/(y_2-y_1)$ respectively. With a discrete data distribution the Discrete Fourier transform is used. When data are arranged in a regular grid, the integrations in eq. (2.11) are calculated as sums and the power spectrum becomes periodic. The highest frequency which may be estimated depends on the spacing of the data, Δx and Δy, since the smallest wavelength is equal to two times the spacing, which on a sphere corresponds to harmonic degree $\pi/\Delta x$ and $\pi/\Delta y$.

For details on the application of the Fourier transform cf. Bracewell (1983), and Meskó (1984).

Eq. (2.6) and eq. (2.16) express the covariance function in a spherical and a plane approximation respectively. In a local area these approximations converge to each other and there exists a link between the degree variances and the power spectrum (Forsberg, 1984a)

$$\sigma_i(R_B/R)^{2i+2} = (i+1/2)1/(2\pi R)\phi((i+1/2)/R) \qquad (2.17)$$

where R is the distance from the center of the earth to the plane. The left hand side expresses the degree variances in eq. (2.6) on a sphere with radius R.

Normalized potential degree variances are obtained as dimensionless quantities through a division by $(GM/R)^2$.

The local covariance function can be determined in two ways. The first method is to evaluate eq. (2.1) using eq. (2.3) or eq. (2.5). The other method is to evaluate eq. (2.1) (given in planar coordinates) using the Discrete Fourier transform and an azimuth-average. The advantage of the second method is that the amount of computation is much smaller than in method one, and that the power spectrum is obtained during the computations. The disadvantage is that the data have to be arranged in a regular grid.

2.2 Estimation of a local empirical covariance function

Before a set of observations is used in studies of the gravity field, it is important that non-gravimetric signals like orbit errors and sea surface topography in altimeter data, are removed from the observations. Furthermore, the observations must be associated with the same geodetic reference system.

Then the longwavelength part of the gravity field has to be removed in order to estimate the local empirical covariance function. If this is done using a spherical harmonic approximation, residual observations, $\hat{y}_i = L_i(T)-L_i(T_N)+n_i$, where n_i is the noise associated with the i'th observation, are obtained. Such quantities are normally used in studies of the gravity field, but an estimation of a local covariance function will result in a covariance function, $\mathrm{cov}(\hat{y},\hat{y}')$, that is affected by the noise of the

observations , and errors in the spherical harmonic approximation (Rapp, 1985). That is

$$\mathrm{cov}(\hat{y},\hat{y}') = \mathrm{cov}(y,y') + \mathrm{cov}(L(T_{ref}-T_N),L'(T_{ref}-T_N)) + \mathrm{cov}(n,n') \qquad (2.18)$$

where $\mathrm{cov}(y,y')$ is the local empirical covariance function, $C(\psi)$, $\mathrm{cov}(L(T_{ref}-T_N), L'(T_{ref}-T_N))$ is the covariance function associated with errors in the spherical harmonic approximation, and $\mathrm{cov}(n,n')$ is the covariance function associated with the noise of the observations. The remaining terms are assumed to be zero. Therefore, the estimated covariance function is not the local empirical covariance function, because $\mathrm{cov}(L(T_{ref}-T_N))$ is associated with wavelengths longer than the extent of the local area. $\mathrm{Cov}(L(T_{ref}-T_N), L'(T_{ref}-T_N))$ is indeed a part of the covariance function that should be used in e.g. collocation, but it is not a part of the local covariance function and can never be estimated from observations in the local area. Remaining long wavelength parts of the gravity field will interfere with the result and furthermore cause spectral leakage if periodicity if assumed. Consequently remaining long wavelength parts of the gravity field have to be removed completely from the observations. $\mathrm{Cov}(n,n')$ is zero for $\psi > 0$, if the noise is assumed to be uncorrelated. For $\psi=0$ $\mathrm{cov}(n,n')$ is equal to the variance of the noise.

In a local area remaining long wavelength parts of the gravity field may appear as a bias. In Knudsen (1987) such a bias was removed in order to center the observations by a transformation into locally best fitting reference system. However, all wavelengths in the spherical harmonic approximation may contain errors. Therefore it is not sufficient to remove a bias. The procedure must be able to consistently remove all wavelengths longer than the extent of the local area from several kinds of gravity field related quantities. A method that fulfills these requirements in least squares collocation using a

covariance function that is designed for the task. Then $\bar{x}_i = L_i(T_{ref}-T_N)$ is estimated from $\bar{y} = \{L_j(T_{ref}-T_N)+n_j\}$ by

$$\bar{x}_i = C_{\bar{x}}^{I} \, (C+D)^{-1} \, \bar{y} \tag{2.19}$$

and

$$e^2 = C_{\bar{x}_i,\bar{x}_i} - C_{\bar{x}_i}^{I}(C+D)^{-1}C_{\bar{x}_i} \tag{2.20}$$

where C is a matrix containing the covariance between the elements in $\bar{y}$, D is a matrix containing the associated error covariances. $C_{\bar{x}_i}$ is a vector holding covariance values between the estimate and $\bar{y}$ and $C_{\bar{x}_i,\bar{x}_i}$ is the variance of the quantities $\bar{x}$, e is the error of $\bar{x}_i$.

In a spherical harmonic expansion the remaining long wavelength part of the gravity field is expressed by a series up to degree and order N. The covariance function between quantities related to this part of the gravity field is expressed by eq. (2.6) but truncated at degree N. If a spherical harmonic approximation up to degree and order M has been subtracted, where M is less than N, the degree variances from the global empirical covariance function (see Tscherning and Rapp (1974)) are used from degree M+1 to N. The quantities $L_j(T_{ref}-T_N)$ are estimated from the observations, $\hat{y}_i$, by a convolution with a filter that truncates the spectrum at harmonic degree N. This has to be done in the space domain, because the long wavelengths are not resolved in the frequency domain. As discussed in Jekeli (1981), a rectangular filter is not a good choice, since the spectrum of this filter has relatively large sidelobes. However, no expression for the ideal filter is given. In the plane the ideal isotropic filter is expressed by a first order Bessel function. A reasonable alternative to the rectangular filter is a rectangular sinc filter: $w(x,y)=\mathrm{sinc}(\frac{x}{\pi} N)\ \mathrm{sinc}(\frac{y}{\pi} N)$, where $\mathrm{sinc}(a)=\sin(\pi a)/(\pi a)$.

Values associated with several kinds of gravity field related quantities may be used in the computations simultaneously. This means that quantities,

$\bar{x}_i$, associated with different kinds of gravity field related quantities are estimated consistently. It is also possible to compute corrections to the spherical harmonic expansion (Tscherning, 1974).

The Fortran program GEOCOL (Tscherning, 1985) can be used for the estimation of the long wavelength part of the gravity field, but a few changes are needed. The subroutine COVAX shall be called with LSUM = .TRUE., N2 is equal to the degree N, and HMAX = -1.0 (see input 7 in the program). Furthermore the constant A (in eq.(2.7)) shall enter CCI(8) directly without being calculated from the variance of gravity anomalies. In the subroutine the array SM must have a dimension of at least N.

The local empirical covariance function may then be estimated, when the remaing long wavelength parts of the gravity field are removed. In principle this covariance function is expressed by an infinite sum of a series of Legendre polynomials, but in practice it is estimated from discrete observations using numerical integration. A reasonable result can only be obtained if the spectrum tends to zero and the spacing between the observations is so small that aliasing effects caused by the higher frequencies are negligible. Since the gravity field is unknown, it is impossible to determine how dense the observations are needed. Therefore the spacing between the observations has to be determined from experiences from other investigations.

A global empirical covariance function was estimated by Tscherning and Rapp (1974). Then, the degree-variances were modelled using eq. (2.7), and the factor A and the radius of the Bjerhammar sphere were adjusted in order to fit the covariance function to the empirical covariance function. The procedure resulted in a depth to the Bjerhammar sphere, $R-R_B$, of 1.22 km. Results from later investigations indicate that this depth should be larger.

For the Canadian covariance function a depth of 3.35 km was found by Schwarz and Lachapelle (1980). In the Faeroe Islands region a depth of 3.17 km was found by Knudsen (1987). In Germany, however, a depth of 1.00 km was found by Denker and Wenzel (1987).

Other studies have been carried out, where the decay of the potential degree variances has been estimated from the power spectrum. Such studies indicate (see e.g. Rapp, 1985, and Forsberg, 1987) that values around -3.6 are typical, but values ranging from -3.3 to -4.8 were found in local studies of the gravity field in the nordic countries.

In order to compare the results obtained by adjusting R_B and the decay of the potential degree-variance, the decay of the degree variance model multiplied by $(R_B/R)^{2i+2}$ was computed. Since $(R_B/R)^{2i+2}$ tends faster to zero than a polynomium, the decay was computed in interval as the difference between the logarithms of the degreee variances multiplied by $(R_B/R)^{2i+2}$ at harmonic degree 180 and 1800. With a depth to the Bjerhammar sphere of 1.0, 2.0, 3.0, and 4.0 km. a decay of -3.2, -3.4, -3.6, and -3.8 was found. Therefore, a depth to the Bjerhammar sphere of 3.0 km agrees quite well with values of the decay around -3.6. However, depths around 1.5 km (corresponding to decays around -3.3) may occur as well as larger depths to the Bjerhammar sphere.

The covariance function models described above may then be used to evaluate how dense the observations need to be distributed in order to estimate the local empirical covariance function. Degree-variances associated with different kinds of obsevations may be calculated and information about how fast they tend to zero is obtained. Also covariance values, C_N, may be computed from different harmonic degrees to infinity (Tscherning, 1976) and information about the magnitude of the high frequency part of the gravity

field is obtained. Such values have been computed for geoid heights and gravity anomalies with a depth to the Bjerhammar sphere of 1.5 km and 3.0 km. In this case the gravity field above harmonic degree 180 is assumed to be studied, so the values are given relative to the values at degree 180 in dB ($10\log_{10}(\sigma_N/\sigma_{180})$ and $10\log_{10}(C_N/C_{180})$) for degree 360, 720, 1440, and 2880 (see Table 1).

$(R-R_B)$	N	σ/σ_{180}		C_N/C_{180}	
		(ζ,ζ)	$(\Delta g,\Delta g)$	(ζ,ζ)	$(\Delta g,\Delta g)$
1.5	360	- 9.17	- 3.13	- 6.45	- 1.54
	720	-18.82	- 6.74	-13.59	- 3.70
	1440	-29.26	-11.16	-21.73	- 6.88
	2880	-41.21	-17.08	-31.72	-11.83
3.0	360	- 9.54	- 3.50	- 7.03	- 2.08
	720	-19.92	- 7.85	-15.13	- 5.27
	1440	-31.84	-13.74	-25.09	-10.65
	2880	-46.73	-22.60	-38.43	-18.36

Table 1. Values of degree-variances, σ_N, and variances, C_N, in dB relative to values at degree 180. Values associated with geoid heights, (ζ,ζ), and gravity anomalies, $(\Delta g,\Delta g)$, are calculated using the Tscherning/Rapp model 4 and a depth to the Bjerghammar sphere, $R-R_B$, of 1.5 km and 3.0 km. The variances are calculated as the sum of the respective degree-variances from harmonic degree N to infinity.

First of all, the results illustrate that the degree-variances associated with geoid heights, tend much faster to zero than the degree-variances associated with gravity anomalies. Furthermore, the degree-variances associated with a depth to the Bjerhammar sphere of 3.0 km tend to go faster to zero than the degree-variances associated with a depth of 1.5 km. The part of the variance that is located above the different harmonic degrees tend to zero in a manner similar to the degree-variances, but not so fast. This shows that if a harmonic degree is determined so the degree-variances have decreased to a certain level, then the variance above this harmonic degree has not decreased to this level. Therefore the spacing that is necessary to resolve the spectrum of the gravity field with negligible aliasing effects

should be determined considering the variance values. If the level is chosen to be between -15 dB and -20 dB the variance of that part of the spectrum that causes the aliasing has decreased to 1%-3%. Then, values associated with a depth to the Bjerhammar sphere of 3.0 km for a harmonic degree of 720 is found for geoid heights and 2880 is found for gravity anomalies. This means that geoid heights and gravity anomalies are needed with a spacing of 1/4° and 1/16° respectively, in order to resolve the two kinds of gravity fields. If a depth of the Bjerhammar sphere is assumed to be 1.5 km a more dense distribution is needed for both kinds of observations.

In order to compute covariance values using eq. (2.5), the local area is subdivided into small cells and one observation in each cell is selected in order to obtain a more homogenously distributed data set with a spacing close to the one that is required. Also, data outside the area should be used. Periodicity may be assumed, but then problems due to wavelengths that are not periodic may arise. As discussed in Knudsen (1987), estimated values should not be filled in empty cells.

If the covariance function is computed using the discrete Fourier transform and an azimuth average, the observations have to be gridded. This can be done using least square collocation. However, faster methods like weighted means and collocation using only the closed observations may be used. The gridding procedure may have a considerable smoothing effect (Knudsen, 1987), which can be diminished by using a much more densely distributed set of observations than the resulting grid.

Before the Fourier transform is calculated, it is advisable to apply a cosine tapered window in order to avoid spectral leakage caused by wavelengths that are not periodic in the local area.

A cosine taper being effective on K points from each border is

A cosine taper being effective on K points from each border is

$$w_k = w_{N+1-k} = \begin{cases} \frac{1}{2} - \frac{1}{2}\cos(\pi \frac{k-1}{K}) & \text{for } k=1,\ldots,K \\ 1 & \text{for } k=(k+1),\ldots,N/2 \end{cases} \qquad (2.21)$$

where N is the number of points in each direction.

The loss of power may be re-established through a multiplication factor, so agreement with the variances before and after the cosine tapering is obtained. That is

$$y^w_{i,j} = c\, y_{i,j}\, w_i\, w_j \qquad (2.22)$$

where c is the multiplication factor

$$c^2 = \sum_{i,j} y^2_{i,j} \;/\; \sum_{i,j} (y_{i,j}\, w_i\, w_j)^2 \qquad (2.23)$$

where $y^w_{i,j}$ are the so-called windowed observations.

Figure 1 and 2 show the effects of using a cosine taper. In both figures, the power spectra (in dB) of a one-dimensional discrete Fourier transform of a sequence of 64 points are shown, when cosine tapers with K=0 (do nothing), K=8, K=16, or K=32 are used. Figure 1 shows the results where a cosine with the frequency f_o=16 was used as sequence. Then the Fourier transforms of the tapers centered at f=16 are obtained, since the multiplication in the space domain corresponds to a convolution in the frequency domain. These frequency domain impulse responses show how the impulses are smoothened out, when K increases. The shoulders, however, appearing with values smaller than -20 dB, become more narrow. With K=32, a cosine taper similar to the Hanning taper is obtained, which in the frequency domain has the values 1/4, 1/2, 1/4 at the frequencies -1,0,1 (*see eg.* Mesko, 1984).

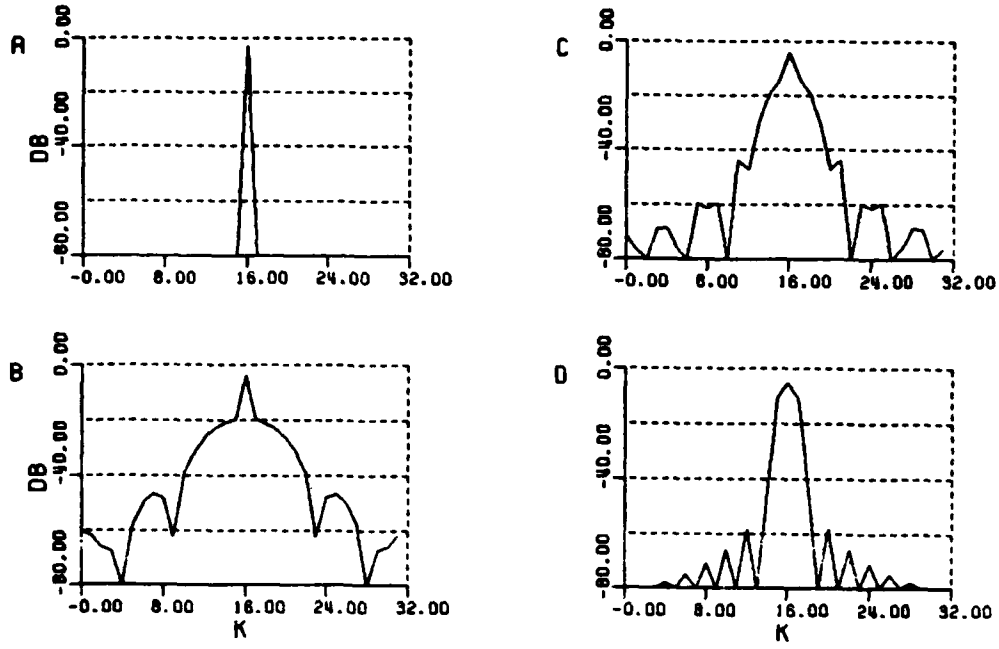

Figure 1. Effect of cosine taper with K=0 (A), K=8 (B), K=16 (C), and K=32 (D) on the discrete power spectrum of a cosine function having a frequency of 16.0 sampled in 64 points.

Figure 2 shows how spectral leakage occurs and decreases when a cosine taper is applies. A function that consists of 10 cosines with the frequencies: f_o = 15.6,...,16.5 having the same amplitude (0.1) was used as sequence. The power of this sequence is expected to be located at f=16 with some influence on the neighboring frequencies. If no cosine taper is applied, it is seen (figure 2A) how those frequencies are resolved in the discrete spectrum. Most of the power (93.0%) is located at f=15, 16, and 17, but the remaining power (7.0%) appears at all frequencies as a result of the leakage effects. When the cosine tapers are applied the leakage effects decrease and the parts of the power that are located as f=15, 16, and 17 increase to 93.8%, 96.0%, and 99.4%. This means that the cosine taper with K=32 (=N/2) results in a spectrum with a minimum frequency dispersion.

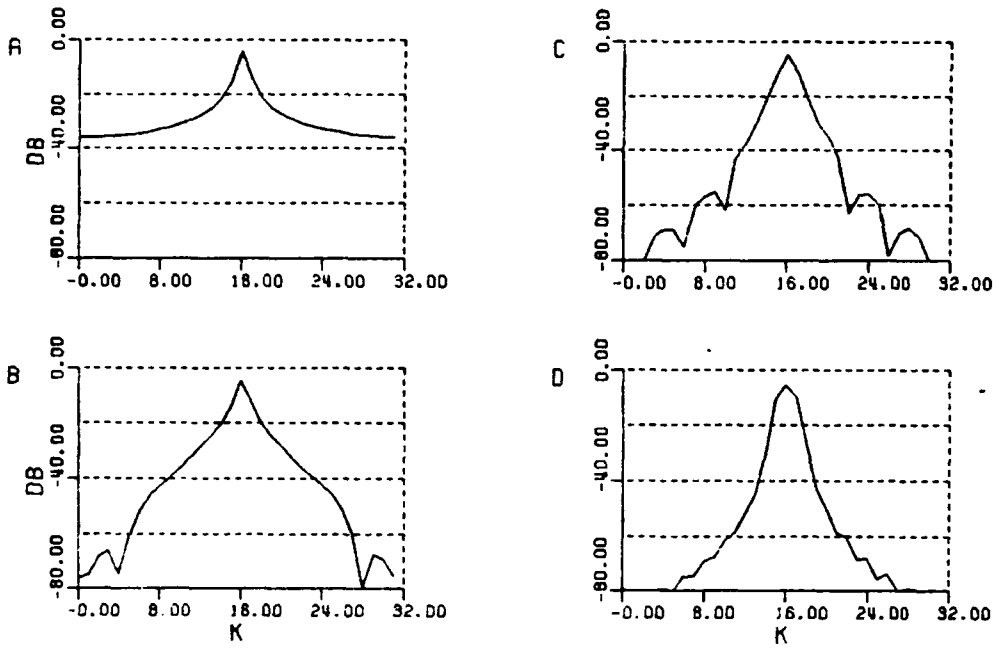

Figure 2. Effect of cosine taper with K=0 (A), K=8 (B), K=16 (C), and K=32 (D) on the discrete power spectrum of a sum of 10 cosine functions having frequencies of 15.6-16.5 sampled in 64 points.

The estimated covariance function contains both the local empirical covariance function and a covariance function associated with the noise. In the power spectrum, uncorrelated noise will appear as a constant level (white noise) and dominate the higher frequencies, where the power of the gravity field is small. The noise in itself is unknown, but the variance of the noise may be estimated if reliable noise terms are associated with the observations. Another possibility is to estimate the noise level in the power spectrum. Then the estimated variance of the noise is subtracted from the estimated covariance function and the local empirical covariance functions associated with the earth's gravity field is obtained.

2.3 The adjustment of a covariance function model

The adjustment of a covariance function model is an important step when the local empirircal covariance function is used in estimations of gravity field related quantities. In Knudsen (1987) the Tscherning/Rapp model was fitted to the empirical covariance values by adjusting the depth to the Bjerhammar sphere, $(R-R_B)$, the factor A, and a scale factor, a, associated with the error degree variances using an iterative least squares inversion procedure. In each iteration, the adjustment of the parameters x_o were calculated as

$$x - x_o = (A^T C_y^{-1} A + C_x^{-1})^{-1} A^T C_y^{-1} (y-y_o) \qquad (2.24)$$

where

x	is the adjusted parameter
y	is the empirical covariance values
y_o	is the values from the model using x_o
A	is the Jacobian matrix $\{\partial y_i/\partial x_j\}$
C_y	is the error covariance matrix of y
C_x	is the covariance matrix of $(x-x_o)$

The ablility of the model to describe the empirical values, or the fitness, was measured by the dimensionless Q value, where

$$Q^2 = \frac{1}{(n-m)} (y-y_o)^T C_y^{-1} (y-y_o) \qquad (2.25)$$

where n is the number of data and m is the number of parameters (=3).

In practice the adjustments were calculated relatively as dimensionless quantities by multiplying each column in matrix A by the associated parameter. Consequently, both the rows and columns in matrix C_x were divided by the associated parameters obtaining relative apriori variances.

The error covariance matrix, C_j, was assumed to be diagonal and contained the square of some empirical error estimates. These errors were calculated in order to evaluate the accuracy of numerical integration in eq. (2.5) and depends on the variances, C_o and C_o' of the observations y and y', the size of the local area, the size of the cells, $\Delta\phi$ and $\Delta\lambda$, and the actual number of

products that would appear if one observation is located in each and every cell. The error, err_k, associated with the k'th covariance value is then

$$err_k = \frac{C}{\sqrt{n_o}} \frac{n_k}{N_k} \tag{2.26}$$

where

$$C = \sqrt{C_o C_o}$$

$$n_k = \begin{cases} \dfrac{(\phi_2-\phi_1)}{\Delta\phi} \dfrac{(\lambda_2-\lambda_1)}{\Delta\lambda} & \text{for } k=0 \\ n_o 2\pi \dfrac{(\psi_k+\psi_{k-1})}{2} \dfrac{(\psi_k-\psi_{k-1})}{\Delta\phi\Delta\lambda} & \text{for } k > 0 \end{cases}$$

The method was tested in the Faeroe Islands region using three combinations of empirical covariance values as input. The results showed that the scale factor, a, was not well determined from gravity anomaly covariance values, and the depth to the Bjerhammar sphere was not well determined from geoid height covariance values only. A combination of these two kinds of covariance values resulted in a well determined model: $(R-R_B)=3.17 \pm 0.34$ km, $A=889 \pm 47\ 10^3 m^4/s^4$, and $a=0.21 \pm 0.04$. Changes in the initial model were not found to have influence on the results.

If agreement between the extent of the area and the degree, which the gravity field have been removed up to, exists, the scale factor should be zero. This was not the case in the Faeroe Islands region. The scale factor was not zero because the remaining longwavelength parts were not completely removed by the centering that was used. Furthermore, the area was larger than the wavelengths that were removed. Suppose that a spherical harmonic expansion up to degree M had been subtracted from the observations, and that remaining long wavelength parts have been removed up to degree N (N<M) using the procedure described in section 2.2. N corresponds to the size of area. Then the degree variances up to degree N are zero. The degree variances between degree N and M are a part of the local covariance function and they may be modelled by the error degree variances that are associated

and they may be modelled by the error degree variances that are associated with the spherical harmonic expansion, multiplied by a scale factor.

The use of a local covariance function model from degree N+1 and a global covariance function model up to degree N, when quantities like $\hat{y}$ is used, is discussed in section 2.2. The local covariance function is also of interest in estimation methods like point mass modelling. Forsberg (1984a) describes the relations between least squares collocation and point mass modelling and how the depth to the point masses affects the shape of the covariance function. A covariance function with an asymptotic decay of the potential degree variances of -3 on the surface of a Bjerhammar sphere (like the Tscherning/Rapp model) is implicitly obtained when a certain distribution of point masses is located at a depth, which is two times the depth to the Bjerhammar sphere.

3. The Use of Satellite Altimeter Data for Estimation of Local Empirical Covariance Functions

In this chapter three local empirical covariance functions are estimated from locally crossover adjusted Seasat/Geos-3 altimeter data. The purpose of a local crossover adjustment is described in a brief discussion on the use of satellite altimetry and the results from the adjustments of the altimeter data are evaluated. Covariance functions associated with the gravity field above harmonic degree 180 are estimated and the spherical harmonic expansion OSU81 (Rapp, 1981) are used as reference. The effects of remaining long wavelength parts on the estimation of empirical covariance functions are studied by comparing covariance functions estimated before and after those remaining long wavelength parts of the gravity field were removed from the observations.

In order to study the variability of the gravity field the three local

areas were selected with different characteristics. Area 1 (The New England Seamount Area: $38° < \phi < 40°$, $295° < \lambda < 297°$) was selected as a 'mild' area, Area 2 ($34° < \phi < 36°$, $294° < \lambda < 296°$) was selected as a 'smooth' area, and Area 3 (The Bermuda Area: $31° < \phi < 33°$, $294° < \lambda < 296°$) was selected as a 'rough' area.

3.1 The Crossover Adjustment

From satellite altimeter data sea surface heights are derived using the ellipsoidal heights of the satellite. These sea surface heights may have been corrected for a number effects (instrumental and atmospherical effects and sea state related bias). From such instantaneous sea surface heights mean sea surface heights are obtained by subtracting variations in the sea surface heights due to tide and variations in the atmospheric pressure. After a removal of the sea surface topography observations of geoid heights are obtained. The accuracy of such observations depends on the quality of the models that have been used in the corrections of the altimeter data. Furthermore the observations contain unmodelled phenomena like effects from rain, clouds, and changes in ocean currents. A geoid height observation derived from an altimetric observation may therefore be described by

$$h = \zeta + \Delta h_c + \Delta h_t + n \qquad (3.1)$$

where ζ is the geoid height and the non-gravimetric signal is divided into a constant part, Δh_c, and a time varying part, Δh_t. n is the noise of the observation.

From a set of observations, $\{h_i\}$, located in a local area, a quantity x may be estimated by least squares collocation

$$x = C^T_{xh} \, (C_{hh} + D)^{-1} \, \{h_i\} \qquad (3.2)$$

where C_{xh} is a vector containing covariance values between x and the observations and C_{hh} is a matrix containing covariance values between the

observations. D is the covariance matrix associated with the noise of the observations. The covariance values associated with the observations depend on the covariances between the ζ, the Δh_c, and the Δh_t terms in eq. (3.1), and the quantity x may be associated with at least one of those terms. A separation of the geoid and the constant part of the non-gravimetric signal will only be successfull if the spectral characteristics of the two signals are different, and a separation of the time varying components will only be successfull if observations, where the constant parts of the signal (including the geoid) are strongly correlated, are available. The first criterion may be fulfilled if the constant part of the non-gravimetric signal consists of long wavelengths and those wavelengths have been subtracted from the gravity field related part of the signal. The second criterion may be fulfilled if repeat observations are used.

The need of repeat observations, when quantities are estimated using eq. (3.2) from observations containing time varying components, may result in very large equation systems and problems in solving them. It is therefore desirable to remove the time varying components from the observations so repeat observations no longer are needed. The problem is then to estimate the time varying components, because the repeat observations still are needed in this step. In this case a solution is obtained by using the differences between the repeat observations. That is using eq. (3.2) and pairs of observations, h_i and h'_i, where h_i and h'_i are located at the same point on either colinear arcs or crossing arcs

$$\begin{aligned} f(t) &= C_{\xi}^{I}\, A^{T}\, A^{T^{-1}}\, (C_{hh}+D)^{-1}\, A^{-1}\, A\, \{h_i,\, h'_i\} \\ &= C_{\xi}^{I}\, A^{T}\, (A(C_{hh}+D)A^{T})^{-1}\, \{d_i\} \\ &= C_{\xi}^{I}\, A^{T}\, (C'+D')^{-1}\, \{d_i\} \end{aligned} \qquad (3.3)$$

where f(t) is the estimate of Δh_t in eq.(3.1). $\{d_i\}=A\{h_i, h'_i\}$ is a set of differences $d_i=h_i-h'_i$. If the time varying components are uncorrelated with the constant terms (ζ and Δh_c) C_t contains the covariance values $cov(\Delta h_t(t), \Delta h_{ti})$ and $cov(\Delta h_t(t), \Delta h'_{ti})$ and C' contains the covariance values $cov(\Delta h_{ti}, \Delta h_{tj}) + cov(\Delta h'_{ti}, \Delta h'_{tj}) - cov(\Delta h_{ti}, \Delta h'_{tj}) - cov(\Delta h'_{ti}, \Delta h_{tj})$. D' contains the error variances of the differences d_i. The error of the estimated value is expressed by

$$err^2(t) = c - C_t^T A^T (C' + D')^{-1} A C_t \qquad (3.4)$$

where c is the variance of the time varying components.

After the time varying components are estimated the altimeter data are corrected and crossover adjusted observations are obtained. That is

$$\begin{aligned} h_a &= h - f(t) \\ &= \zeta + \Delta h_c + n_a \end{aligned} \qquad (3.5)$$

where n_a is the noise of the crossover adjusted observation.

The method and how the covariance values may be computed are discussed in Knudsen (1987a). Tests in The Faeroe Islands Region using the adjusted Seasat altimeter data (Liang, 1983) showed that remaining time varying components were successfully removed. It was assumed that orbit related errors had been removed and that the main part of the remaining variations was caused by an inaccurate ocean tide model and the unmodelled phenomena mentioned above. The covariance values where calculated using a gaussian function and the along track distance between the crossover points. As correlation distance 1000 km was used.

The potential of this method is that altimeter data in local areas with inaccurate ocean tide models (coastal areas like the Mediterranean) can be adjusted more accurately than in conventional bias or bias/tilt adjustments. On the other hand it is not felt that the method is suitable for orbit error

estimations, since orbit errors are geographically correlated (see eg. Engelis, 1987). Further studies of time varying components and their correlations are needed and can for example be based on the extensive repeat information made available through the Geosat mission.

3.2 Results from the Crossover Adjustment of Seasat/Geos-3 altimeter data.

For the estimation of the local empirical covariance functions observations from the merged Seasat/Geos-3 data set (Liang, 1983) were used. All observations in each 2° x 2° area plus a 2° border zone were retrieved. It resulted in three data sets each containing 35000 (approximately) observations. Since the observations were distributed far more densely than needed, it was decided to thin out the data. During this process a cell size of 1/6° by 1/6° was chosen for the estimation of the empirical covariance functions (explained in the next section). Then a subset of arcs were selected, so the observations associated with those arcs would provide at least one observations in each cell. This was done in each area and resulted in data sets each containing 12000 observations approximately.

Crossover discrepancies were computed as the difference in height between ascending and descending tracks. The heights and the position were calculated by a linear interpolation between the four neighboring observations. The crossover adjustments were carried out using the method described in section 3.1. It was assumed that orbit errors had been removed and a covariance function similar to the one used in the Faeroe Islands Region was used. Since the number of crossover discrepancies was large, the estimation of the time varying components was based on crossover discrepancies between Seasat arcs, and crossover discrepancies between Seasat and Geos-3 arcs only. RMS values of the discrepancies were computed before and after the

adjustments. These values are shown in Table 2.

The results from the crossover adjustments (Table 2) show that discrepancies between Seasat arcs generally are much smaller than discrepancies between Geos-3 arcs. The reason for that is that the Seasat altimeter data are much more accurate than the Geos-3 altimeter data. The results show furthermore that the discrepancies after the adjustments are largest in Areas 1 and smallest in Area 3. It was also expected, since Area 1 is located in the center of an area with large sea surface variations due to changes in the Gulf Stream (Menard, 1983). Those variations may contain a rather short wavelength signature, which is not completely modelled in the adjustment.

Area	Type	Number	RMS[a]	RMS[b]
1	S/S	134	0.41 m	0.15 m
	S/G	1014	0.52 -	0.34 -
	G/G	1737	0.60 -	0.58 -
2	S/S	106	0.25 m	0.13 m
	S/G	964	0.48 -	0.31 -
	G/G	2084	0.60 -	0.54 -
3	S/S	111	0.13 m	0.09 m
	S/G	1064	0.37 -	0.27 -
	G/G	2322	0.51 -	0.46 -

Table 2. Results of the crossover adjustments in Area 1, 2, and 3 extended with a border zone of 2 degrees. The number and RMS values before (a) and after (b) the adjustments of discrepancies between Seasat arcs (S/S), between Seasat and Geos-3 arcs(S/G), and between Geos-3 arcs (G/G).

Crossover adjusted altimeter data were obtained using eq. (3.5) and their noise terms were evaluated. The purpose of an evaluation of the noise terms is to determine whether they are appropriate geoid observation noise terms or not. As mentioned in section 3.1 the accuracy depends on the quality of the terms associated with the data do not take this into account. From studies of repeat tracks by Marks and Sailor (1986) typical geoid noise terms of 8 cm for

Seasat and 28 cm for Geos-3 altimeter data were found. These values are approximately 40% higher than the typical errors of 6 cm and 20 cm that are assigned Seasat and Geos-3 altimeter data respectively. In this case the noise terms are evaluated using RMS values of the crossover discrepancies divided by the errors of the discrepancies. If the numbers are larger than one, time varying components are still present. Such remaining time varying components are correlated along track, but across track they may be treated as uncorrelated errors. If the correlations along track are small, the total errors may be assumed to be uncorrelated. Consequently the noise terms can be modified, so they agree with the magnitude of the crossover discrepancies. This was done in each area by computing scale factor for the noise terms of Seasat and Geos-3 respectively. Then the noise terms were multiplied by the respective scale factors and noise terms associated with geoid height observations were obtained. The scale factors and RMS values of the modified noise terms are shown in Table 3.

Area	Seasat		Geos-3	
	factor	RMS	factor	RMS
1	1.58	0.11 m	2.03	0.41 m
2	1.45	0.09 -	1.96	0.39 -
3	1.00	0.06 -	1.46	0.29 -

Table 3. Scale factors and RMS values of the modified noise terms for Seasat and Geos-3 in Area 1, 2, and 3.

3.3 The Estimation of the Local Empirical Covariance Functions.

It was decided to estimate local empirical covariance functions associated with harmonic degrees greater than 180, which roughly corresponds to wavelengths shorter than 2 degrees, and use the space domain method with observations selected in cells covering the areas. The size of the local areas

areas should be taken into account within distances of 2°. Then covariance values are calculated using eq. (2.5) by forming averages of products between observations in the local 2° by 2° areas and observations in the 6° by 6° areas. It corresponds to a typical estimation situation, where quantities in a local area are estimated from observations in the local area and a border zone. The variances of the modified noise terms are also calculated and subtracted from the variances of the observations.

The cell size was determined from the results in section 2.2 and from results by Marks and Sailor (1986). The results from section 2.2 showed that a cell size of 1/4° would be sufficient to resolve geoid heights. Marks and Sailor, however, found that the short wavelength resolution limit is about 32 km for Seasat and about 60 km for Geos-3. These wavelengths corresponds roughly to sample spacings of 1/7° and 1/4° (half wavelength). Since a combination of Seasat and Geos-3 data are used, a cell size of 1/6° was chosen. Then each area was subdivided into cells of 1/6° by 1/6° and one observation in each cell were selected from the locally crossover adjusted altimeter data.

The removal of the information content of wavelengths longer than the extent of the local areas was in the first place done by subtracting the contribution from the spherical harmonic expansion OSU81 up to degree and order 180. Then empirical covariance functions were estimated. This was done in order to study the effects of remaining long wavelength parts.

Then remaining long wavelength parts were estimated using the method described in section 2.2. Mean values were computed using a rectangular sinc filter on a 1/2° by 1/2° grid covering each 6° by 6° area. From these mean values remaining long wavelength parts in the observations were estimated by least squares collocation (eq. (2.19)) and a covariance function truncated at

least squares collocation (eq. (2.19)) and a covariance function truncated at degree 180. The variances of the mean values were smaller than the error variance of OSU81 (1.15 m^2), so constant non-gravimetric effect were assumed to be small and included in the estimated values, since those effects mainly are due to sea surface topography of wavelengths corresponding to harmonic degrees smaller than 180. After a removal of the estimated values from the crossover adjusted altimeter data, observations of geoid heights associated with harmonic degrees greater than 180 were obtained. Then local empirical covariance functions were estimated from these space domain highpass filtered observations.

The estimated geoid height variances in the three local areas were 0.256 m^2, 0.372 m^2, and 1.899 m^2 respectively, before the remaining long wavelength parts (after the subtraction of the OSU81 field) were removed. (Noise variances of 0.069 m^2, 0.090 m^2, and 0.033 m^2 respectively have been subtracted.) Using the highpass filtered observations these numbers reduced to 0.213 m^2, 0.112 m^2, and 1.217 m^2. The variances associated with the remaining long wavelength parts are then 0.043 m^2, 0.260 m^2, and 0.682 m^2 or 20%, 232%, and 56% relative to the variances of the highpass filtered observations. The effects of the remaining long wavelength parts on the estimation of the geoid height variances are therefore considerable. Especially the results obtained in Area 2, where the magnitude of the remaining long wavelength parts is more than twice as big as the magnitude of the highpass filtered observations, show the importance of removing those long wavelength parts.

The local empirical covariance functions estimated in Area 1, Area 2, and Area 3 using the selected observations before and after the removal of the remaining long wavelength parts are shown in Figure 3-5. Furthermore power

spectra calculated from 1/6° by 1/6° mean values using a cosine taper (eq. (2.21)) with K=6 are shown. The purpose of calculating power spectra was to evaluate the spectral content at the lower frequencies, so no attempts to correct for effects due to smoothing and noise were made. The local areas were extended to 4° by 4° in order to estimate the 1/4 cycle/degree power also. The effects from the remaining long wavelength parts are also seen by comparing the two covariance functions in each area. Before the highpass filtering the covariance functions in Area 1 and Area 2 have their first zero crossing at lags of 1.75 deg. and more than 2.00 deg. respectively. After the highpass filtering the first zero crossings occurs at lags close to 0.5 deg. The power spectra show the different spectral contents. Before the highpass filtering the observations contain large signals associated with frequencies 1/4 and 1/2 cycles/degree, which efficiently are removed from the highpass filtered observations. The information contents of wavelengths longer than the extents of the local areas have therefore been removed from the highpass filtered observations. Consequently the covariance functions calculated from those highpass filtered observations are estimates of the local empirical covariance functions associated with the gravity field above harmonic degree 180.

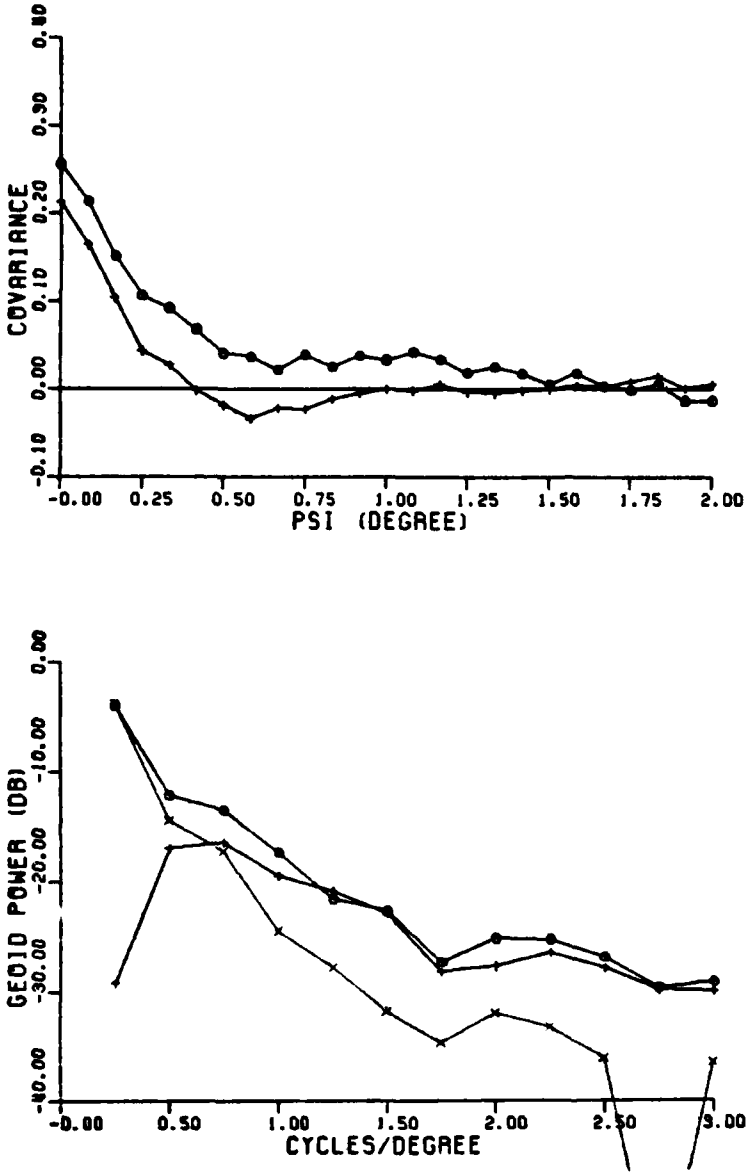

Figure 3. Upper: Local empirical covariance functions calculated in Area 1 from altimeter data minus OSU81 (o) and from high-pass filtered altimeter data (+) (units in m^2). Lower: Power spectra calculated in Area 1 from 10'x10' mean values of altimeter data minus OSU81 (o), high-pass filtered altimeter data (+), and their differences (x).

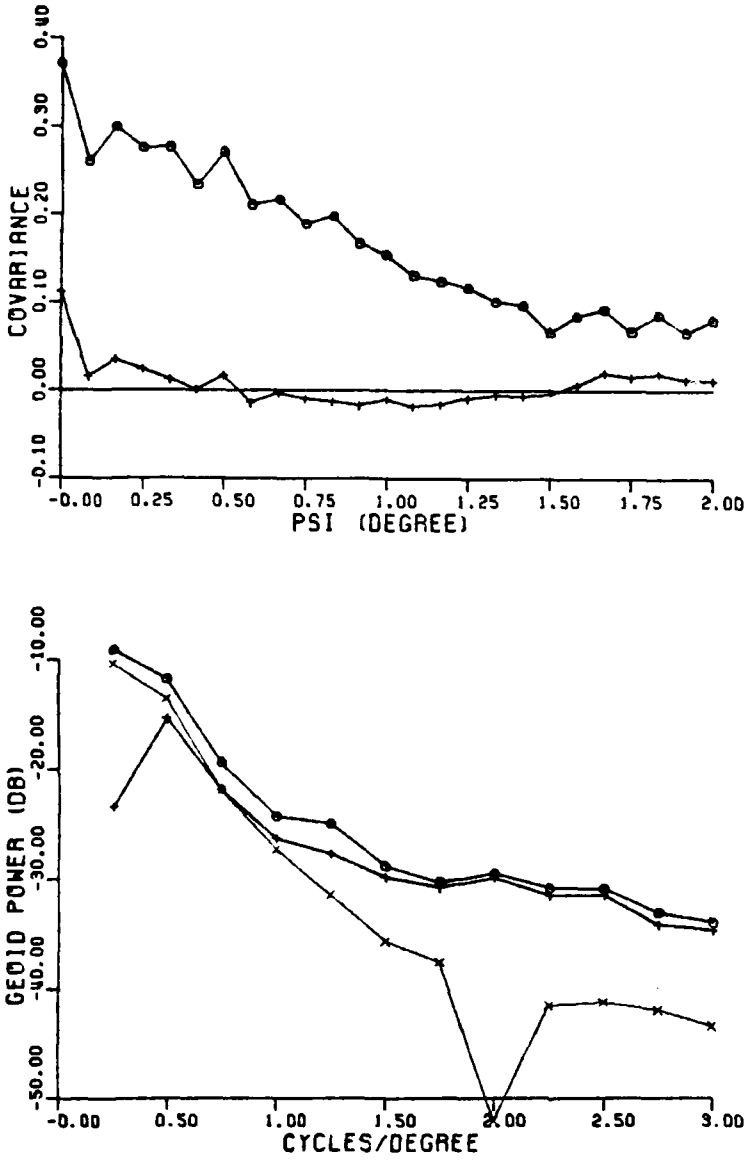

Figure 4. Upper: Local empirical covariance functions calculated in Area 2 from altimeter data minus OSU81 (o) and from high-pass filtered altimeter data (+) (units in m^2). Lower: Po.er spectra calculated in Area 2 from 10'x10' mean values of altimeter data minus OSU81 (o), high-pass filtered altimeter data (+), and their differences (x).

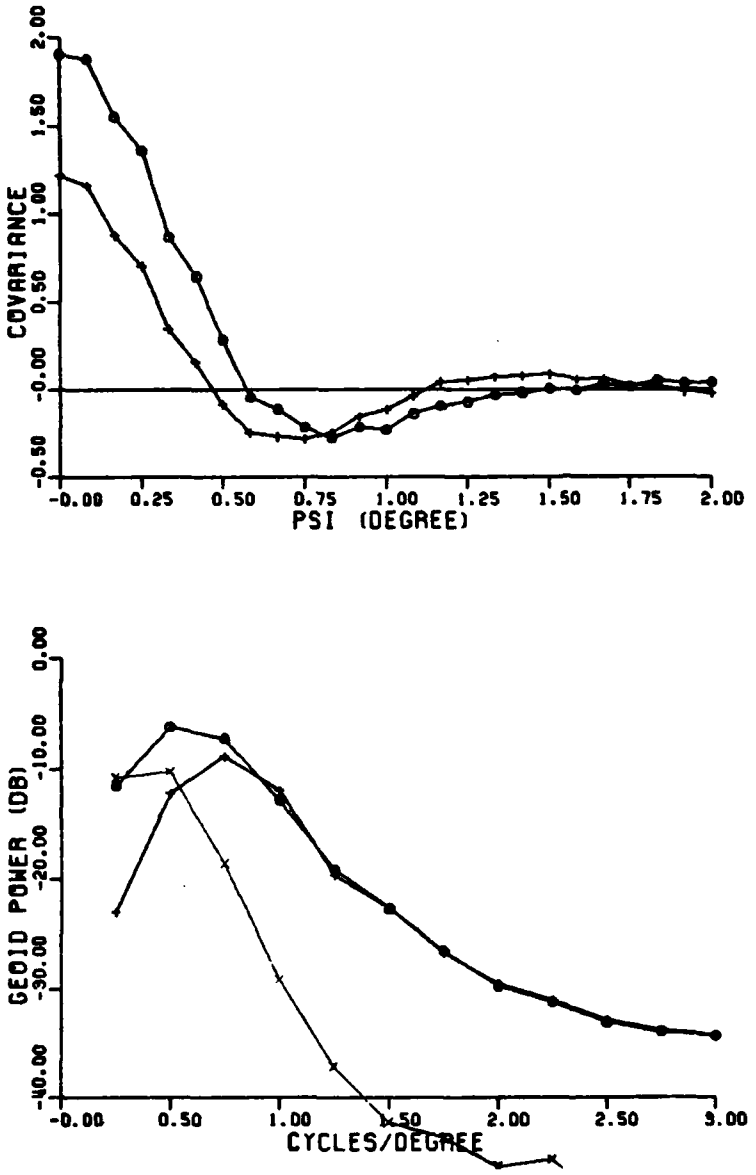

Figure 5. Upper: Local empirical covariance functions calculated in Area 3 from altimeter data minus OSU81 (o) and from high-pass filtered altimeter data (+) (units in m^2). Lower: Power spectra calculated in Area 3 from 10'x10' mean values of altimeter data minus OSU81 (o), high-pass filtered altimeter data (+), and their differences (x).

4. Local Empirical Covariance Functions from Residual Terrain Reduced Altimeter Data.

The effect from the topography is a considerable part of the gravity field and, as far as the topography is known, this effect can be used when the gravity field is modelled. This may be done by computing gravity field related quantities from the topography and subtract the terrain effects from the observations. Then terrain reduced observations are used in the estimations and the results are obtained by adding the estimated quantities and the terrain effects. If a spherical harmonic expansion is used as reference, terrain effects associated with the same wavelengths as the harmonic expansion are removed implicitly. Then residual terrain effects are used. Methods for computing residual terrain effects from a digital terrain model using rectangular prisms or Fourier techniques are desribed in e.g. Forsberg (1984) and Forsberg (1985).

The effect of using topographic information is that the magnitude of the unknown parts of the gravity field becomes smaller. Furthermore strongly varying gravity fields in mountainous areas reduce to more smooth gravity fields. These effects are described in Forsberg (1986), where results from a study of the spectral properties of the gravity field in the Nordic countries are evaluated. RMS values of gravity anomaly observations relative to GPM-2 (Wenzel, 1985) to degree and order 180 were calculated in 38 2° x 4° blocks before and after residual terrain effects were removed from the observations. In Figure 6 the RMS values of the observations relative to GPM-2 (FA: Residual Free-air Anomalies) are plotted against RMS values of the residual terrain reduced observations relative to GPM-2 (BA: Residual Bouguer corrected Anomalies). Furthermore the distribution of the two types of RMS values are shown. The RMS values of the residual free-air anomalies range

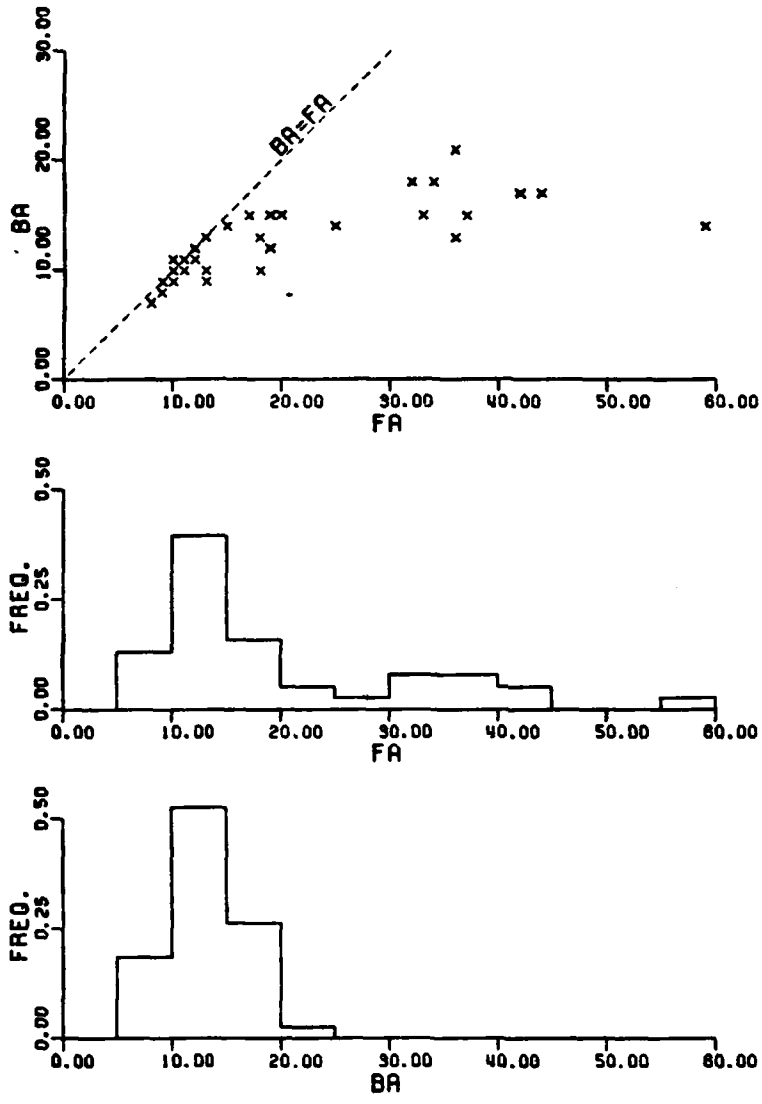

Figure 6. Plot of variances of free-air anomalies (FA) against variances of Bouguer corrected anomalies (BA) calculated by Forsberg (1986) in the Nordic countries. Also the distributions of the two types of variances are shown.

from 8 mgal to 59 mgal. Typical values of 10-15 mgal were found in lowland areas in Denmark and Finland, and typical values of 30-45 mgal were found in mountainous areas in Norway. The RMS values of the residual Bouguer corrected observations range from 7 mgal to 21 mgal. The mean value of the RMS values dropped from 19.3 mgal to 12.3 mgal, and the standard deviation of the RMS values dropped from 12.5 mgal to 3.3 mgal, when the residual terrain effect were removed. Areas with smooth gravity fields and smooth topography did not change much, but the rough areas became much smoother. The most dramatic change was found in a Norweigian Block, where the RMS value dropped from 59 mgal to 14 mgal. The gravity field in the Nordic countries has thereby become much more homogeneous, and the magnitude of unknown parts of the gravity field did decrease.

In this chapter a method for computing residual terrain effects from an isostatic earth model is described. The method is used in the three local areas described in the previous chapter and local empirical covariance functions are estimated from residual terrain reduced altimeter data. Furthermore correlations between the altimetric and bathymetric geoid undulations are evaluated.

4.1 Calculation of Residual Geoid Undulations from an Isostatic Earth Model.

Since the earth is believed to be about 90% isostically compensated, it was decided that the computation of geoid undulations from the topography should take the isostasy into account. Therefore an isostatic earth model was needed. A simple (and highly idealized) model is the Airy-Heiskanen model (Heiskanen and Moritz, 1967). This model is based on a floating theory, where the topography is compensated at a depth of 30 km by root/antiroot formations at the crust/mantle interface. Seismic results indicate that the depth to the

crust/mantle interface is correlated with the topography, which may justify the principle of an isostatic compensation at the crust/mantle interface. The Airy-Heiskanen model, however, assumes a strictly local compensation, which more likely has a regional character due to the elasticity of earth materials. The Vening Meinesz model assumes such a regional compensation and is a "smeared out" version of the Airy-Heiskanen model. Even though the Vening Meinesz model is more realistic than the Airy-Heiskanen model, the compensation mechanisms are much more complicated. Experiments by Lewis and Dorman (1970) suggests that the compensation takes place at different levels depending on the wavelengths of the topography.

It was decided to use an isostatic Airy-Heiskanen model assuming that a gravity field similar to the gravity field from a Vening Meinesz regional model is obtained by increasing the depth of compensation. An increase of the depth of compensation corresponds to a smoothing of the crust/mantle topography by an upward continuation. Then the depth to the crust/mantle interface is given by

$$d' = D_c - \alpha d \qquad (4.1)$$

where d is the bathymetric depth, D_c is the depth of compensation, and $\alpha=\Delta\rho_t/\Delta\rho_c$. $\Delta\rho_t$ is density constant associasted with the topography and $\Delta\rho_c$ is the crust/mantle density contrast. As densities of ocean water, crust, and mantle values of 1.03 g/cm^3, 2.67 g/cm^3, and 3.27 g/cm^3 were assumed. Then $\Delta\rho_t$=1.64 g/cm^3, $\Delta\rho_c$=0.60 g/cm^3, and α=2.73.

The computation of geoid undulations associated with wavelengths shorter than 2° was done using Fourier techniques in a flat earth approximation as described in Forsberg (1985). The constant parts of the topography and the compensating masses were omitted, since they are meaningless in a flat earth approximation (The geoid undulation becomes infinite). Then a geoid

undulation outside the masses may be expressed by

$$N_I = \frac{T_T+T_C}{\gamma} \tag{4.2}$$

where γ is the normal gravity, T_T is the potential from the terrain

$$T_T = G\Delta\rho_t \int_A \int_{d_o}^{d} \frac{1}{r}\, dz dA \tag{4.3}$$

and T_C is the potential from the compensating masses

$$T_C = G\Delta\rho_t \int_A \int_{d'_o}^{d'} \frac{1}{r}\, dz dA \tag{4.4}$$

G is gravitational constant, d_o is the mean depth in an area A, and $d'_o = D_c - \alpha d_o$.

A first-order expansion of $1/r$ around d_o in eq. (4.3)

$$1/r(z) = 1/r_o - d_o/r_o^3 (z-d_o), \quad r_o^2 = (x_Q-x_p)^2 + (y_Q-y_p)^2 + d_o^2$$

results in

$$\begin{aligned} T_T &= G\Delta\rho_t \int_A \int_{d_o}^{d} \left(\frac{1}{r_o} - \frac{d_o}{r_o^3}(z-d_o)\right) dz dA \\ &= G\Delta\rho_t \int_A \left[\left(\frac{1}{r_o} + \frac{d_o^2}{r_o^3}\right)(d-d_o) - \frac{d_o}{2r_o^3}(d^2-d_o^2)\right] dA \\ &= G\Delta\rho_t \int_A \left[\frac{1}{r_o}(d-d_o) - \frac{d_o}{2r_o^3}(d-d_o)^2\right] dA \end{aligned} \tag{4.5}$$

and for eq. (4.4)

$$T_C = G\Delta\rho_c \int_A \left[\frac{1}{r'_o}(d'-d'_o) - \frac{d'_o}{2r'^3_o}(d'-d'_o)^2\right] dA \tag{4.6}$$

The expressions for the potential (eq. (4.5-4.6)) are now represented as two dimensional convolutions, which are suitable for the use of Fourier techniques, since a convolution becomes a simple product in the frequency domain. The series expansion of $1/r$ that was used in order to obtain this representation, was carried out to first order. A zero-order expansion

corresponds to a condensation of the masses on a layer at mean depth. In a first-order expansion more of the geometry of the topography is taken into account. General expresssions for calculation of potential anomalies Fourier techniques may be found in Parker (1972).

The accuracy of the expressions for the potential depends on the magnitude of high-order terms that are omitted. According to Parker (1972) the magnitude of the high-order terms will be smallest, when the reference level is chosen so $(d-d_o)_{max} = -(d-d_o)_{min}$. Assuming that this level is mean level, this have been done in eq. (4.5) and eq. (4.6). Furthermore the accuracy is highly depending on the roughness of the topography. Tests carried out by Tziavos et al. (1988) in an area with a very rough terrain show that the first and the second term in the expansion are sufficient to compute airborne gravity terrain effects with an accuracy of 0.25 mgal. Since geoid undulations are smoother than gravity anomalies, eq. (4.5) and eq. (4.6) are assumed to be sufficiently accurate.

Then geoid undulations, eq. (4.2), are calculated using eq. (4.5) and eq. (4.6), and the relation: $(d'-d'_o) = -\alpha(d-d_o)$

$$N_I = \frac{G}{\gamma}\Delta\rho_t \int_A \left[\frac{1}{r_o}(d-d_o) - \frac{d_o}{2r_o^3}(d-d_o)^2\right] dA$$

$$+ \frac{G}{\gamma\alpha}\Delta\rho_t \int_A \left[\frac{-\alpha}{r'_o}(d-d_o) - (-\alpha)^2\frac{d'_o}{2r'^3_o}(d-d_o)^2\right] dA$$

$$= \frac{G}{\gamma}\Delta\rho_t \int_A \left[\left[\frac{1}{r_o} - \frac{1}{r'_o}\right](d-d_o) - \frac{1}{2}\left[\frac{d_o}{r_o^3} + \alpha\frac{d'_o}{r'^3_o}\right](d-d_o)^2\right] dA \qquad (4.7)$$

The integration in eq. (4.7) are in the form of two convolutions involving $(d-d_o)$ and $(d-d_o)^2$. These convolutions may be performed most efficiently by Fourier transforming complex data:

$$\left[(d-d_o) + i(d-d_o)^2\right] \tag{4.8}$$

and a complex kernel:

$$\left[\left(\frac{1}{r_o} - \frac{1}{r'_o}\right) - i\frac{1}{2}\left(\frac{d_o}{r_o^3} + \alpha\frac{d'_o}{r'^3_o}\right)\right] \tag{4.9}$$

From the computed spectra the spectra of each component may be isolated through the conjugate symmetries of the Fourier transform. The kernel was set to zero at distances larger than 2°, so only inner zone effects were computed. If a border zone larger than 2° is used, problems with non-periodic wavelengths are avoided and windowing are not needed. A maximal distance of 2° was assumed to be sufficient, since only wavelengths shorter than 2° were of interest. From the Fourier transforms of the topography and the kernel, the Fourier transform of the geoid undulations is obtained by a multiplication.

In order to obtain geoid undulations associated with wavelengths shorter than 2°, a high-pass filtering was needed. This was done in the frequency domain before the inverse Fourier transformation. As high-pass filter, $S(\omega)$, a step function, $S_o(\omega)$, was used, which has been smoothed by a Hanning taper $W(\omega)$ in order to take the frequency dispersion into account (Mesko, 1984). That is

$$S_o(\omega) = \begin{cases} 0 & \text{for } \omega<\omega_o \\ 1 & \text{otherwise} \end{cases}$$

and

$$W(\omega) = \begin{cases} \frac{1}{\Delta\omega}\cos^2\left(\frac{\pi}{2}\frac{\omega}{\Delta\omega}\right) & \text{for } |\omega| < \Delta\omega \\ 0 & \text{otherwise} \end{cases}$$

then

$$S(\omega) = \int_{-\infty}^{\infty} S_o(\omega')\, W(\omega'-\omega)\, d\omega'$$

$$\begin{cases} 0 & \text{for } \omega \leq (\omega_0 - \Delta\omega) \\ \frac{1}{2}\left(1 + \frac{\omega-\omega_0}{\Delta\omega}\right) + \frac{1}{2\pi}\sin\left(\frac{\omega-\omega_0}{\Delta\omega}\right) & \text{for } (\omega_0-\Delta\omega) < \omega < (\omega_0+\Delta\omega) \\ 1 & \text{otherwise} \end{cases} \qquad (4.10)$$

where ω is the frequency, $\Delta\omega$ is the frequency spacing, and ω_0 is the cut-off frequency. The cut-off frequency is 0.5 cycle/degree, which roughly corresponds to a harmonic degree of 180.

Then residual geoid undulations, ΔN_I, from the isostatic earth model were obtained using an inverse Fourier transform of the Fourier transform of the geoid undulations multiplied by the high-pass filter, eq. (4.10).

Residual geoid undulations were computed in 5′ x 5′ "SYNBAPS" mean ocean depths was used. This was done using two compensation depths: D_c=-50 km and D_c=-70 km. If the true compensation depth is assumed to be 30 km, this corresponds to a smoothing of the crust/mantle topography by upward continuations of 20 km and 40 km respectively. At the locations of the altimeter data the residual geoid undulations were found by bilinear interpolation in the grids.

4.2 Residual Terrain Reduction of the Altimeter Data and the Local Empirical Covariance Functions.

The residual terrain effects were compared with the high-pass filtered altimetry by evaluating RMS values and power spectra of the quantities. Furthermore correlation coefficients between the two quantities were calculated. The reduction of the altimetry was evaluated in a similar way. Finally local empirical covariance functions were estimated from the terrain reduced altimeter data.

Correlation coefficients between the terrain reduced altimetry and the bathymetric geoid may be used in an evaluation of the earth model. They cannot tell if a model is correct, but they can tell if a model can be better. A

zero correlation is obtained, when that part of the observations that are correlated with the terrain effect, are removed completely. If the correlation coefficient is different from zero, the terrain model may be used more efficiently. A correlation coefficient different from zero may occur if wrong density contrasts are used. Then either too less or too much are removed from the observations, which result in either a positive or a negative correlation coefficient. The use of a wrong compensation depth may have the same effect, since the strength of the signal from the compensating masses hereby changes.

The computed RMS values of the residual bethymetric geoid undulations are generally smaller than the RMS values of the altimetry (see Table 4). Furthermore the values associated with a compensation depth of 50 km are smaller than with a compensation depth of 70 km. The computed correlation coefficients between the altimetry and the bathymetric geoid (Table 5) show that the correlations are largest in Area 3, where the gravity field is rough, and smallest in Area 2, where the gravity field is smooth. A reason for decreasing correlations may be that both the altimetry and the "SYNBAPS" bathymetry contain errors. In smooth areas those errors may dominate the true signals, which results in very small correlation coefficients. Furthermore the isostatic earth models are highly idealized and many geological structures are not taken into account.

Area	ΔN_T		Δh	$\Delta h - \Delta N_T$	
	A	B		A	B
1	0.33 m	0.37 m	0.53 m	0.41 m	0.41 m
2	0.07 -	0.08 -	0.45 -	0.45 -	0.45 -
3	0.86 -	0.96 -	1.12 -	0.42 -	0.41 -

Table 4. RMS values of residual bathymetric geoid undulations, ΔN_T, with compensation depths: D_c=-50 km (A) and D_c=-70 km (B), high-pass filtered altimeter data, Δh, and residual terrain reduced altimeter data in Area 1, Area 2, and Area 3.

Area	$(\Delta h, \Delta N_I)$	$(\Delta h - \Delta N_I, \Delta N_I)$	
	A	A	B
1	0.65	0.05	-0.07
2	0.15	0.00	-0.05
3	0.94	0.45	0.21

Table 5. Correlation coefficients between altimetry, Δh, and bathymetric geoid, ΔN_I, with D_c=-50 km (A), and between terrain reduced altimetry and bathymetric geoid with D_c=-70 km (B) in Area 1, Area 2, and Area 3.

The RMS values of the residual terrain reduced altimetry are approximately the same, and only a slight change in Area 3 is found, when the depth of compensation is changed from 50 km to 70 km. In Area 1 and Area 2 there are practically no correlation between the terrain reduced altimetry and the bathymetric geoid associated with both compensation depths. The altimetry have therefore been reduced as well as possible with both earth models. In Area 3 the terrain reduced altimetry is still correlated with the bathymetric geoid, when a compensation depth of 50 km is used. This correlation is decreased, when a compensation depth of 70 km is used. Since the effects from the masses above sea level of Bermuda are not taken into account when "SYNBAPS" data are used, no further attempts to adjust the earth model in Area 3 were made.

The local empirical covariance functions and power spectra were estimated from the high-pass filtered terrain reduced altimeter data, where the residual terrain effects obtained with a compensation depth of 50 km were used in Area 1 and Area 2, and the residual terrain effects obtained with a compensation depth of 70 km were used in Area 3. These results together with the results obtained before the terrain effects were subtracted, are shown in Figure 7-9.

The power spectra show that the reductions are larger than 50% (=3 dB) at frequencies between 0.75 and 1.75 cycles/degree in Area 1, at 0.75 cycles/degree in Area 2, and between 0.50 and 1.75 cycles/degree in Area 3

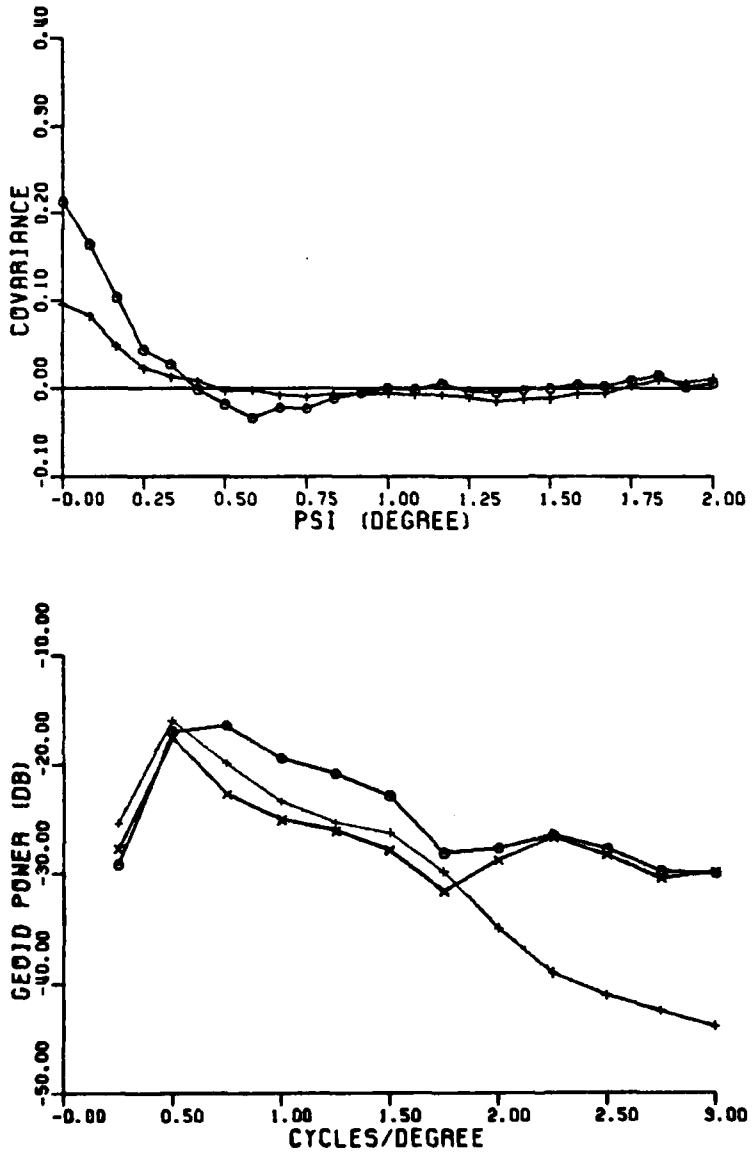

Figure 7. Upper: Local empirical covariance functions calculated in Area 1 from high-pass filtered altimeter data (o) and from residual terrain reduced altimeter data (+) (units in m^2). Lower: Power spectra calculated in Area 1 from 10'x10' mean values of high-pass filtered altimeter data (o), residual terrain reduced altimeter data (x), and bathymetric geoid (+). The bathymetric geoid was calculated using a compensation depth of 50 km. Note that the symbols have changed in the lower figure.

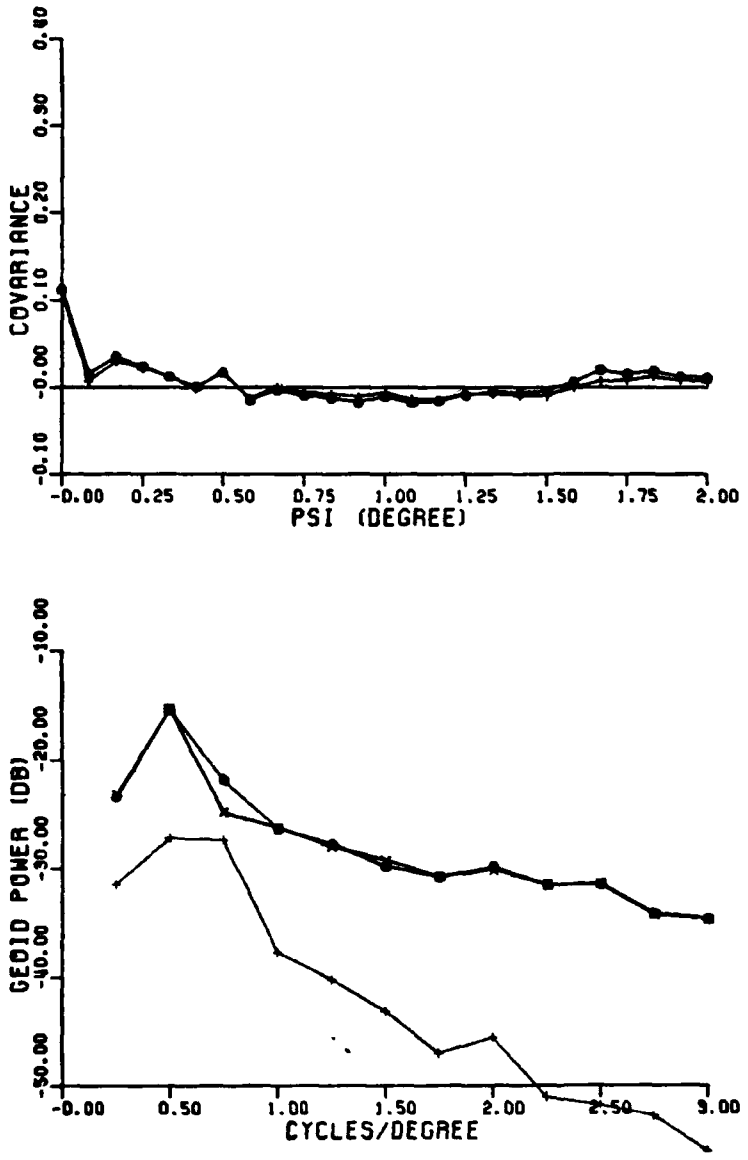

Figure 8. Upper: Local empirical covariance functions calculated in Area 2 from high-pass filtered altimeter data (o) and from residual terrain reduced altimeter data (+) (units in m^2). Lower: Power spectra calculated in Area 2 from 10'x10' mean values of high-pass filtered altimeter data (o), residual terrain reduced altimeter data (x), and bathymetric geoid (+). The bathymetric geoid was calculated using a compensation depth of 50 km.

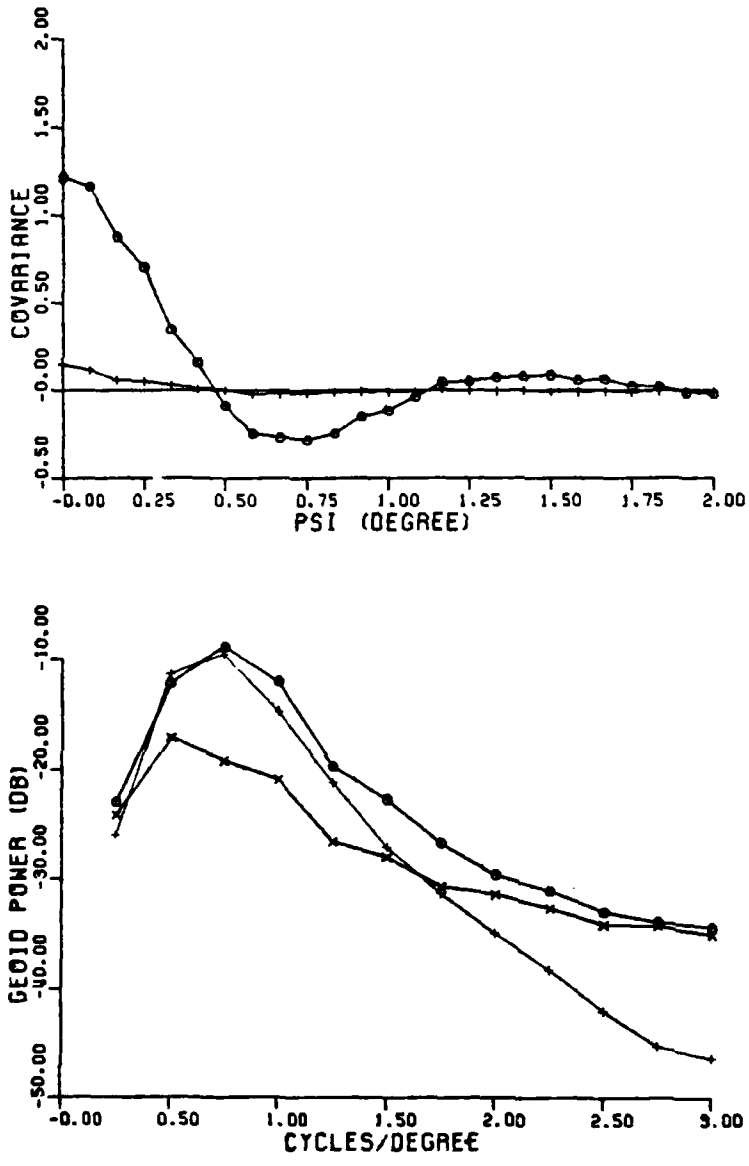

Figure 9. Upper: Local empirical covariance functions calculated in Area 3 from high-pass filtered altimeter data (o) and from residual terrain reduced altimeter data (+) (units in m^2). Lower: Power spectra calculated in Area 3 from 10'x10' mean values of high-pass filtered altimeter data (o), residual terrain reduced altimeter data (x), and bathymetric geoid (+). The bathymetric geoid was calculated using a compensation depth of 70 km.

At higher frequencies the power of the terrain effects is very small compared with the power of the altimetry.

The estimated terrain reduced geoid height variances in the three local areas were 0.096 m^2, 0.108 m^2, and 0.147 m^2 respectively. The largest reduction took place in Area 3 where the geoid height variance decreased 88% (=9.21 dB), when the terrain effects were subtracted. In Area 1 and Area 2 the reduction were 55% (=3.47 dB) and 4% (=0.18 dB) respectively.

The effects of reducing the altimeter data with terrain effects computed from the "SYNBAPS" bathymetry are that the geoid height variances decreased from 0.11-1.22 m^2 to 0.10-0.15 m^2. The magnitude of the unmodelled parts of the gravity field have hereby decreased and the differences between the geoid height variances in the three local area have decreased remarkably. This may be important in a determination of a covariance function model.

5. Determination of Covariance Function Models from Local Empirical Geoid Height Covariance Functions

In least squares collocation a covariance function model that represents the local empirical covariance function, is needed. It is therefore an important step to determine such a model. In section 2.3 a method for adjusting a Tscherning/Rapp model to empirical covariance values is described. In this chapter the use of this method is described, when the estimated geoid height autocovariance values are used.

A determination of a covariance function model from a local empirical geoid height autocovariance function is known to provide a result, where the depth to the Bjerhammar sphere is not well determined (Knudsen, 1987). This has been verified by adjusting a model to the empirical covariance functions estimated from the altimeter data in Area 1, Area 2, and Area 3. Since remaining long wavelength parts of the gravity field have been removed, the

scale factor, a, was fixed to be zero. The results showed that the standard deviations of the estimated depths to the Bjerhammar spheres were about the same magnitude as the parameters themselves.

Since the depth to the Bjerhammar sphere is not well determined from geoid height covariance values only, it was decided to fix this parameter to different depths, and adjust the factor, A, only. Then gravity anomaly variances were calculated from the adjusted covariance function models. The results from the adjustments where covariance values estimated from the altimeter data, before the residual terrain reduction, in Area 1, Area 2, and Area 3 are shown in Table 6-8 respectively.

$R-R_B$	A	Q	$C_{\zeta,\zeta}$	$C_{\Delta g,\Delta g}$
0.5 km	$1195 \cdot 10^3$ (m/s)^4	1.02	0.168 m^2	857 mgal^2
1.0 -	1249 -	1.04	0.166 -	693 -
2.0 -	1359 -	1.07	0.163 -	545 -
4.0 -	1600 -	1.13	0.159 -	416 -
8.0 -	2165 -	1.23	0.152 -	310 -

Table 6. Results from the adjustment of a covariance function model to the empirical covariance function in Area 1 before terrain reduction.

$R-R_B$	A	Q	$C_{\zeta,\zeta}$	$C_{\Delta g,\Delta g}$
0.5 km	$610 \cdot 10^3$ (m/s)^4	1.11	0.086 m^2	437 mgal^2
1.0 -	639 -	1.12	0.085 -	354 -
2.0 -	698 -	1.14	0.084 -	280 -
4.0 -	827 -	1.17	0.082 -	215 -
8.0 -	1140 -	1.22	0.079 -	162 -

Table 7. Results from the adjustment of a covariance function model to the empirical covariance function in Area 2 before terrain reduction.

$R-R_B$	A	Q	$C_{\zeta,\zeta}$	$C_{\Delta g,\Delta g}$
0.5 km	$8530 \cdot 10^3$ (m/s)^4	0.67	1.197 m^2	6111 mgal^2
1.0 -	8727 -	0.68	1.162 -	4842 -
2.0 -	9506 -	0.71	1.143 -	3810 -
4.0 -	11152 -	0.77	1.108 -	2902 -
8.0 -	13463 -	0.89	1.018 -	2078 -

Table 8. Results from the adjustment of a covariance function model to the empirical covariance function in Area 3 before terrain reduction.

The results from the adjustments of covariance function models to the

empirical covariance values (Table 6-8) show that the effects of a dramatic change of the depth to the Bjerhammar sphere from 0.5 km to 8.0 km are quite small, when the Q values and the model geoid height variances are considered. The effect on the model gravity anomaly variance, however, is large. This means that determinations of the depth to the Bjerhammar sphere may be done, if estimated gravity anomaly variances are available. Without other information than the geoid height covariance values the determination of a covariance function model is difficult. Furthermore the gravity fields in the three local areas have different characteristics, so general assumption abouth the gravity fields cannot easily be made.

Then covariance function models were adjusted to fit the empirical covariance values estimated from the residual terrain reduced altimeter data. The potential degree variances associated with the terrain reduced gravity field were also assumed to tend to zero somewhat faster than i^{-3}, so the Tscherning/Rapp model could be used. It is of course a problem to decide, if it is reasonable to model the degree variances associated with the terrain reduced gravity field using a Tscherning/Rapp model. The results obtained by Forsberg (1986) in the Nordic countries, where accurate terrain models are available, justify the use of a Tscherning/Rapp model. If inaccurate terrain models are used, the gravity field will only be reduced at wavelengths longer than the resolution of the terrain models, and the shorter wavelengths will remain unreduced. Then the covariance function model should model the degree variances in a similar way, as if a spherical harmonic expansion had been subtracted. This may be done by using a sort of error degree variances up to a harmonic degree corresponding to the resolution of the terrain model, and a Tscherning/Rapp model above this harmonic degree.

The results from the adjustments of covariance functions associated with

residual terrain reduced gravity fields (Table 9-11) show the same problems as described above. The importance of these results are that the differences between the three local areas have become smaller. The results obtained in Area 1 are very similar to the results obtained in Area 2. In Area 3 the respective variances are about 57% larger than the variances calculated in Area 2. This is probably due to an incomplete modelling of the terrain above sea level.

The major differences between the characteristics of the gravity fields in the three local areas have been removed, which should make it easier to use general assumptions about the gravity field, when covariance function models are determined. Furthermore the magnitude of the unknown parts of the gravity field have decreased, which decreases the effects of using a wrong covariance function model. In Area 3 a change of depth to the Bjerhammar sphere from 2.0 km to 4.0 km results in a change in the gravity anomaly variance corresponding to 7.9 mgal (RMS) without terrain correction and 2.5 mgal (RMS) with terrain correction.

$R-R_B$	A	Q	$C_{\zeta,\zeta}$	$C_{\Delta g,\Delta g}$
0.5 km	$566 \cdot 10^3 (m/s)^4$	0.95	0.079 m^2	406 $mgal^2$
1.0 -	592 -	0.96	0.079 -	329 -
2.0 -	646 -	0.99	0.078 -	259 -
4.0 -	763 -	1.04	0.076 -	199 -
8.0 -	1048 -	1.16	0.073 -	149 -

Table 9. Results from the adjustment of a covariance function model to the empirical covariance function in Area 1 after terrain reduction.

$R-R_B$	A	Q	$C_{\zeta,\zeta}$	$C_{\Delta g,\Delta g}$
0.5 km	$560 \cdot 10^3 (m/s)^4$	1.19	0.079 m^2	401 $mgal^2$
1.0 -	586 -	1.19	0.078 -	325 -
2.0 -	639 -	1.21	0.077 -	256 -
4.0 -	755 -	1.24	0.075 -	196 -
8.0 -	1039 -	1.29	0.072 -	148 -

Table 10. Results from the adjustment of a covariance function model to the empirical covariance function in Area 2 after terrain reduction.

$R-R_B$	A	Q	$C_{\zeta,\zeta}$	$C_{\Delta g,\Delta g}$
0.5 km	$881 \cdot 10^3 (m/s)^4$	0.79	0.124 m^2	632 $mgal^2$
1.0 -	922 -	0.81	0.123 -	512 -
2.0 -	1007 -	0.84	0.121 -	404 -
4.0 -	1192 -	0.89	0.119 -	310 -
8.0 -	1643 -	0.97	0.115 -	234 -

Table 11. Results from the adjustment of a covariance function model to the empirical covariance function in Area 3 after terrain reduction.

Assuming that the decay of the potential degree variances associated with the terrain reduced gravity field is -3.6 corresponds to a covariance function model with $R-R_B$=3.0 km. In Area 1 and Area 2 a model with $A=711 \cdot 10^3 (m/s)^4$ having a gravity anomaly variance of $(15 \text{ mgal})^2$ may be used. In Area 3 the factor A and the variance may be multiplied by 1.57.

In this chapter covariance function models have been adjusted to the local empirical covariance values estimated in the three local areas from altimeter data. The results show that the characteristics of the terrain reduced gravity fields, as observed by the altimeter data, are quite similar. The determination of covariance function models, however, still need more information about the gravity fields than provided by the altimeter data, or generalizations about the gravity fields. In the three local areas covariance function models were determined using the assumption that the decay of the potential degree variances associated with the terrain reduced gravity field is -3.6.

6. Summary and Conclusions

In this report, techniques for the estimation of local empirical covariance functions are described. The importance of removing those parts of gravity field that are associated with wavelengths longer than the extent of the local areas, is explained and a method for doing it is given. Furthermore a technique for the computation of residual geoid heights from an Airy-Heiskanen isostatic earth model is described. Then the use of satellite

altimeter data for the estimation of gravity field related quantities in local areas is evaluated and the variability of the gravity field associated with harmonic degree greater than 180 is studied in three 2°x2° areas by comparing local empirical covariance functions computed from altimeter data before and after a residual terrain reduction. Finally covariance function models are adjusted to fit the local empirical covariance functions.

From the merged SEASAT/GEOS-3 altimeter data relative to OSU81, geoid height observations associated with harmonic degrees greater than 180 were obtained in three steps. In the first step the altimeter data were corrected for time varying components by a crossover adjustment. In the second step remaining long wavelength parts due to errors in OSU81, sea surface topography, and correlated parts of remaining orbit errors were removed by a highpass filtering. In the last step the noise terms associated with the altimeter data were modified in order to obtain noise terms associated with the altimeter data as geoid height observations. The results from the crossover adjustment show that uncorrelated parts of the time varying components in general were well removed. Some short wavelength variations due by changes in the Gulf Stream, however, appeared not to be well modelled in the adjustments. A reason for that may be that a (too) simple covariance function associated with the time varying components was used. The covariance function was originally designed to model sea surface variations having wavelengths of about 1000 km (Knudsen, 1987a), and the variations due to changes in the Gulf Stream have a characteristic wavelength of 550 km and an amplitude up to about 25 cm (Menard, 1983). A more detailed study of the non-gravimetric signals are needed, so covariance functions describing the correlations in space and time between those signals can be determined.

The effects of wavelengths longer than the extent of the local area on an

estimation of a local empirical covariance function were evaluated by comparing empirical covariance functions and power spectra estimated before and after the highpass filtering. The effects were found to be considerable. Especially the results obtained in the "smooth" Area 2 show the importance of removing those long wavelength parts. Here the magnitude of the long wavelength parts is more than twice as big as the magnitude of the highpass filtered geoid heights. In the estimation of the long wavelength parts a smoothing of the observations was done using a rectangular sinc filter. A rectangular sinc function is a better choice than a box-car function, but it is not isotropic. It is felt that the relations between the spherical and the planar representation have to be studied more carefully, so more optimal low-pass filters can be derived.

Residual terrain effects were calculated from "SYNBAPS" 5'x5' mean bathymetry using Fourier techniques. As earth model an isostatic Airy-Heiskanen model was used, but the depth of compensation was increased in order to simulate a regional Vening Meinesz model. Residual terrain reduced altimeter data were computed using compensation depths of 50 km and 70 km respectively. The results show that the reductions of the altimeter data practically are unaffected by the change in compensation depth, when wavelengths shorter than 2° are considered. The important thing is that the RMS values of the altimetry have decreased to about the same level. In the following tests a compensation depth of 50 km was used in Area 1 and Area 2, ans 70 km was used in Area 3, since the smallest correlations between the terrain effects and the terrain reduced altimetry were obtained using these compensation depths.

The results from the comparisons of the local empirical covariance functions and the power spectra calculated from the highpass filtered altimeter

data before and after the residual terrain effects were subtracted, show that the variances are reduced by about 3 dB, 0 dB, and 9 dB in three local areas. As expected the reductions were found to depend on the roughness of the gravity fields, and the estimated geoid height variances decreased to values between 0.10 m^2 and 0.15 m^2, when the terrain effects were removed. The remaining parts of the gravity fields, having a RMS value of about 0.35 m, are not modelled by the Airy-Heiskanen isostatic earth models that were used. The power spectra indicate that only a little reduction took place at frequencies larger than 1.75 cycles/degree. The spectra of the altimetry are influenced by noise, but the spectra of the bathymetric geoids do decrease rapidlly above this frequency. This suggests that the resolution of the "SYNBAPS" bathymetry is about 1.75 cycles/degree (a wavelength of 63 km) and poorer than the resolution of the altimetry, which in chapter 3 was determined to be about 3 cycles/degree (a wavelength of 37 km). Therefore the modelling of the high frequency parts may be improved by using a more accurate bathymetry, but changes in the actual density distribution may also cause high frequency changes in the gravity field.

The results from the adjustments of covariance function models show that more information about the gravity fields than provided by geoid height observations, or strong generalizations are needed, when covariance function models are determined. A removal of the terrain effects, however, removes the major differences between the gravity fields, which should make it easier to use general assumptions about the residual gravity field and, perhaps more important, decrease the effects of using a wrong covariance function model. Therefore the use of terrain effects in gravity field modelling have reduced some of the problems in the determination of a covariance function model. The results, however, may indicate that the accuracy of the terrain model is too

poor to reduce the high frequency parts of the gravity field, which is not taken into account in the covariance function modelling. This explains why the model variances are smaller than the empirical variances. A study of the use of other covariance function models may result in a better description of degree variances associated with the terrain reduced gravity field.

REFERENCES

Bracewell, R.N., The Fourier Transform and its Applications, Second edition, McGraw-Hill, 1978.

Denker, H., and H.G. Wezel, Local Geoid Determination and Comparison with GPS Results, Bulletin Geodesique, V. 61, No. 4, 349-366, 1987.

Engelis, T., Radial Orbit Error Reduction and Sea Surface Topography Determination Using Satellite Altimetry, Report No. 377, Department of Geodetic Science and Surveying, The Ohio State University, Columbus, 1987, NASA Grant NAG5-519.

Forsberg, R., A Study of Terrain Reduction, Density Anomalies and Geophysical Inversion Methods in Gravity Field Modelling, Report No. 355. Department of Geodetic Science and Surveying, The Ohio State University, Columbus, 1984, AFGL-TR-84-0174; ADA150788.

Forsberg, R., Local Covariance Functions and Density Distributions, Report No. 356, Department of Geodetic Science and Surveying, The Ohio State University, Columbus, 1984a, AFGL-TR-84-0214; ADA150792.

Forsberg, R., Gravity Field Terrain Effect Computations by FFT, Bulletin Geodesique, 59, 342-360, 1985.

Forsberg, R., Spectral Properties of the Gravity Field in the Nordic Countries, Bulletin Geodesie Sci. Aff., Anno XLV, No. 4, 361-383, 1986.

Goad, C.C., Tscherning, C.C., and Chin, M.M., Gravity Empirical Covariance Values for the Continental United States, Journal of Geophysical Research, Vol. 89, No. B9, 7962-7968, 1984.

Heiskanen, W.A., and H. Mortitz, Physical Geodesy, W.H. Freeman, San Francisco, 1967.

Jekeli, C., Alternative Methods to Smooth the Earth's Gravity Field, Report No. 327, Department of Geodetic Science and Surveying, The Ohio State University, Columbus, 1981, NASA Grant No. NGR 36-008-161.

Knudsen, P., Estimation and Modelling of the Local Empirical Covariance Function using Gravity and Satellite Altimeter Data, Bulletin Geodesique, Vol. 61, 145-160, 1987.

Knudsen, P., Adjustment of Satellite Altimeter Data from Cross-over Differences Using Covariance Relations for the Time Varying Components Represented by Gaussian Functions, Proceedings of the IAG Symposia, International Association of Geodesy, Paris, 617-628, 1987a.

Lewis, B.T.R., and L.M. Dorman, Experimental Isostasy 2. An Isostatic Model for the U.S.A. derived from Gravity and Topographic Data, Journal of Geophysical Research, Vol. 75, No. 17, 3367-3386, 1970.

Liang, C., The Adjustment and Combination of Geos-3 and Seasat Altimeter Data, Report No. 346, Department of Geodetic Science and Surveying, The

Ohio State University, Columbus, 1983, NOAA Grant No. NA80AA-D-0070.

Marks, K.S., and R.V. Sailor, Comparison of Geos-3 and Seasat Altimeter Resolution Capabilities, Geophysical Research Let., Vol. 13, No. 7, 697-700, 1986.

Menard, Y., Observations of Eddy Fields in the Northwest Atlantic and Northwest Pacific by SEASAT Altimeter Data, Journal of Geophysical Research, Vol. 88, No. C3, 1853-1866, 1983.

Mesko, A., Digital Filtering: Applications in Geophysical Exploration from Oil, Pitmman Advanced Publishing Program, Pitman Publishing Ltd., London, 1984.

Moritz, H., Advanced Physical Geodesy, Herbert Wichmann Verlag, Karlsruhe, 1980.

Nash, R.A., and S.K. Jordan, Statistical Geodesy - An engineering perspective, Proceed. of the IEEE, Vol. 66, No. 5, 532-550, 1978.

Parker, R.L., The Rapid Calculation of Potential Anomalies, Geophysical Journal of the Royal Astronomical Society, 31, 447-455, 1972.

Rapp, R.H., The Earth's Gravity Field to Degree and Order 180 Using Seasat Altimeter Data, Terrestrial Gravity Data, and other Data, Report 322, Department of Geodetic Science and Surveying, The Ohio State University, Columbus, 1981, AFGL-TR-82-0029; ADA113098.

Rapp, R.H., Detailed Gravity Anomalies and Sea Surface Heights Derived from Geos-3/Seasat Altimeter Data, Report No. 365, Department of Geodetic Science and Surveying, The Ohio State University, Columbus, 1985, AFGL-TR-85-0191; ADA166593.

Sanso, F., Statistical Methods in Physical Geodesy. In: Suenkel, H., Mathematical and Numerical Techniques in Physical Geodesy, Lecture Notes in Earth Sciences, Vol. 7, 49-155, Springer-Verlag, 1986.

Schwarz, K.P., and G. Lachapelle, Local Characteristics of the Gravity Anomaly Covariance Function, Bulletin Geodesique, 54, 21-36, 1980.

Schwarz, K.P., Data Types and their Spectral Properties. In: Schwarz, K.P., Local Gravity Field Approximation, The University of Calgary, Alberta, No. 6i0003, 1-66, 1985.

Suenkel, H., N. Bartelme, H. Fuchs, M. Hanafy, W.D. Schub, and M. Wieser, The Gravity Field in Austria. In: The Gravity Field in Austria, Edited by the Austrian Geodetic Commission, Geodaetische Arbeiten Oesterteichs Fur die International Ermessung, Neue Folge, Band IV, 47-75, 1987.

Tscherning, C.C., and R.H. Rapp, Closed Covariance Expressions for Gravity Anomalies, Geoid Undulations, and Deflections of the Vertical Implied by Anomaly Degree Variance Models. Report No. 208, Department of Geodetic Science and Surveying, The Ohio State University, Columbus, 1974, AFCRL-TR-74-0231; ADA786417.

Tscherning, C.C., A Fortran 4 Program for the Determination of the Anomalous Potential Using Stepwise Least Squares Collocation, Report No. 212, Department of Geodetic Science and Surveying, The Ohio State University, Columbus, 1974, AFCRL-TR-74-0391; ADA006362.

Tscherning, C.C., Covariance Expressions for Second and Lower Order Derivatives of the Anomalous Potential, Report No. 225, Department of Geodetic Sciences and Surveying, The Ohio State University, Columbus, 1976, AFGL-TR-76-0052;ADA024720.

Tscherning, C.C., Local Approximation of the Gravity Potential by Least Squares Collocation. In: Schwarz, K.P.: Local Gravity Field Approximation. The University of Calgary, Alberta, No. 60003, 277-361, 1985.

Tscherning, C.C., GEOCOL - A FORTRAN program for gravity field approximation by Collocation, Technical Note, Geodaetisk Institut, 3. ed., 25. March, 1985a.

Tscherning, C.C., Functional Methods for Gravity Field Approximation. In: Suenkel, H.: Mathematical and Numerical Techniques in Physical Geodesy, Lecture Notes in Earth Sciences, Vol. 7, 3-47, Springer-Verlag, 1986.

Tziavos, I.N., M.G. Sideris, R. Forsberg, and K.P. Schwarz, The Effect of the Terrain on Airborne Gravity and Gradiometry, Journal of Geophysical Research, Vol. 93, No. B8, 9173-9186, 1988.

Wenzel, H.G., Hochaufloessende Kugelfunktionsmodelle fuer das Gravitationspotential der Erde. Wiss. Arb. Fachrightung Vermessungswesen der Universitaet Hannover, No. 137, 1985.